Journal of Mechanical Engineering and Research Developments

Volume - 13

Issue- 1

Jan - Apr 2025

ENRICHED PUBLICATIONS PVT.LTD

JE - 18,Gupta Colony, Khirki Extn,
Malviya Nagar, New Delhi - 110017.
E- Mail: info@enrichedpublication.com
Phone :- +91-8877340707

Journal of Mechanical Engineering and Research Developments

Aims and Scope

Subject areas include, but are not limited to the following fields:

- Aerodynamics
- Aerothermodynamics
- Automotive Engineering
- Computer Aided Engineering
- Component Manufacturing
- Conveyors
- Energy Studies
- Engines and Turbines
- Engineering Education

Journal of Mechanical Engineering and Research Developments

Journal of Mechanical Engineering Research and Developments

(Volume No. 13, Issue No. 1, January - April 2025)

Contents

Microstructural Variations in Electron Transparent Areas of a Rapidly Solidified High Speed Tool Steel

M. Nasrul Haque*, D. H. Kirkn'ood
*** Departmcnt of Metailurgical Engineering, B"tJ'E-'T" Dhaka,
** Deportrnent of Metailurgy, University of Sheffield' Shefficld, U'K.

ABSTRACT

Tl high speed steel (having C = 0."76Va,W = 17 .8V0, Cr = 3.87Vo andY=0.987o) has been rapidly solidified by the two-piston technique. Thin areas (which are transparentto electronbeam) of rapidly solidified splatshavebeenexamined ly rransmiision electron microscopy. The microsffuiture indicates that solidification occurs in the plane of the splat surface and not perpendicular to it. These ai"a, ur" foundto contain d-ferrite, austenite and martensite. d - ferrite areas are mainly observed with segregation of carbide along clendritic boundaries. The areas which are solidified without segregation of carbide are found to decompose spinodally at room temperature. Austenite is observed either free from segregation or with segregation of carbicle aiong cen foundaries. The areas where the segregation of carbide is more are found as maflensite at room lempcraturc'

INTRODUCTION

Rapid solidification has been a field of vigorous research activity in recent years, where molten metal is directly quenched in contact wilh a solid substrate' Very high ctoiing rate can be achieved if a very thin layer of molten metal is brought in a good contact with the substrate (1). The areas of a rapidly solidified splat which are transparent to electron beam' being extremcly thin, have bcen consiclered to have cooled fastest in gun fechnique (2)' It has been postulated that the direction of hcat florv is towards the n"orJtt contact point on the substrate and that heat extraction and hence soliclification takes place in the plane of the splat/substrate interface(3)' Varieties of microstructures har,c becn rcportcd (4) in the electron uansparent areas de.pencling on thevariations of alloy cornposirions' Depending on the variation in solidification condition it might be expected to observe microstructural variations in elecFon ransparent areas. The present investigation is an attempt to investigate the variations in microstructure at different places in tlle electron transparellt areas on the sane material
(Tl high speed tool steel) due to variation in cooling condition.

EXPERIMENTAL METHOD

Splats of T1 high speed steel wcrc produced from molten droplcts heated to around 28000C by the twopiston technique described elsewhere(5). Electron fransparent areas u'cre observed near the edge of the splas' Those areas wcre examined by transmission electron microscopy at an operating voltage of 100 KV.

EXPERIN{ENTAL RESULTS

Fig.l(a) shows an electron trans-parent area containing all cl -fcrrite denclrites. Fig' 1(b) is a micrograph from r-he above area at higher magnification showing precipitation of carbide at the inter dendritic boundaries' This microstructure is similar to that of d-fenite dendrites obser ved by Sare and Honeycombe(6) in electron transparent area of rapidly solidified Ml high speed steei. 'A' on the microgrgph @ig.1ft))represents the centre of nucleation, at which the solid phase first nucleared and grew in the plane of the splat, indicating that heat extracaion had raken place in thatplane. The centres of nucleation ofd-fenite dendrites in Fig. 1(a) are very close (-1.5 pm) ro each orher and the cellular arm spacing is found to be -0.15 pm. Only in a few areas d-ferrite was found without any precipitation of carbide and those areas are observed to decompose spinodally (Fig.2) giving rise to streaks on rhe electron diffraction pattern. Fig. 3 shows another electron lransparent area containing all austenite grains. These grains re r&ql fut to grow in the plane of the splat. The microsnrflec Mil_ cates that the austenite grains growing from bqh slfia* mwl a[a common line. Initially the austenitegrains gran nrdh:tur any precipitation of carbide and selected area d,rtihrrumm pafterns from those areas do not show an-v sF0(:;:m. i second phase, buf towards the end of solidifi cadon a ielfui.s structure is apparent with linear arrays of precipim* n uhe cel1 bounclaries.

In some eiectron transparent areas twinned marten_ill!-'r4s observed (Fig.a). These areas are found to contain l:;i-”

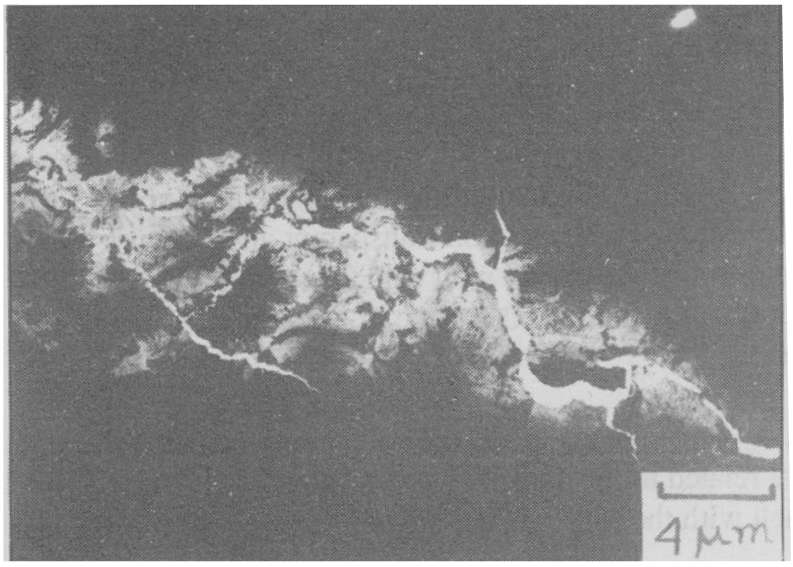

Fig. 1(a) Transmission eiectron rnicrogrlpli having all d-fenite dendrites.

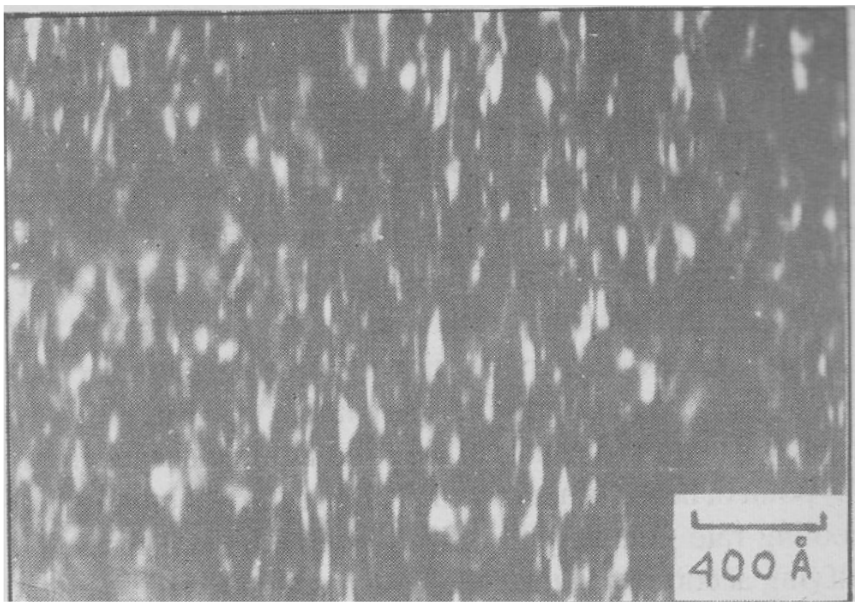

Fig.2 Transrnission electron micrograph containing d-ferrite rvhich apears to have decomposed spinodally.

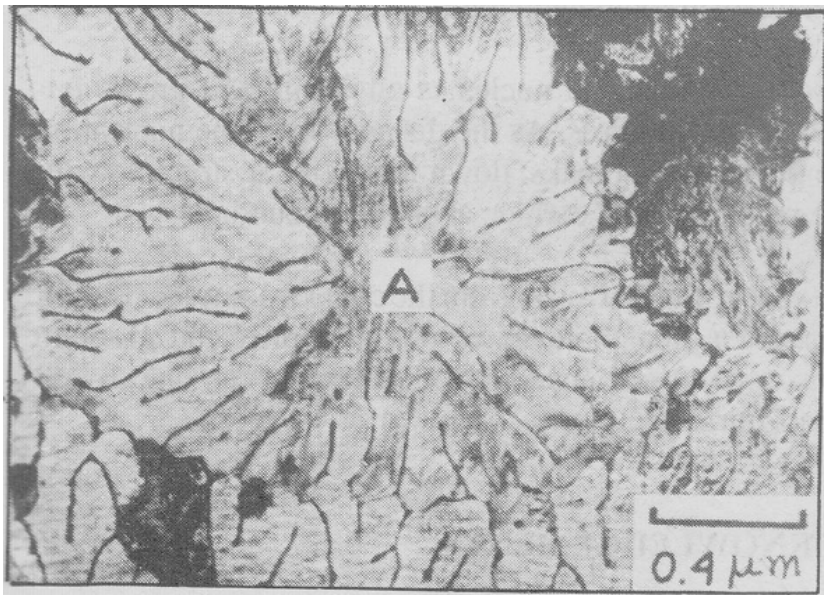

Fig. 1(b) Micrograph from the above area at higher magnification showing precipitation of carbide at the interdendritic boundaries.

Fig.3 Transmission electron micrograph having all austenite grains.

number of coarse particles. Electron diffraction showed that those particles are MuC carbide. Those areas initially solidified as austenite with segregation of MuC carbide and transformed to twinned mmtensite at ambient temperature.

DISCUSSION

It has been shown previously(7) that in rapid solidification of Tl high speed steel, solidification starts with the nucleation of d-fenite at those points in direct contact with the subsffate. Austenite then nucleates on ferrite as a results of changing thermal'conditions or of solute rejection and build-up at the solidliquid interface. Austenite then grew as a primmy phase of solidification. If the points of contact with the substrate (i.e. the centres of nuclei) are very close the melt. may completely solidify as d-ferrite before tlte austenite could nucleate @ig. 1(a)). On the other hand Fig.3 is found to contain only austenite grains. The micrograph indicates that the nuclealion sites are outside this transparent area. Comparing this micrograph with the microstructure of the outer surface layer of the thicker region of splat(7) suggests that d-fenite first nucleated (outside this fansparent area) in contact with the substrate followed by nucleation of austenite. Initially the austenite grows as partitionless, without any carbide precipitation. As the distance of the solidliquid interface from the point ofheat extraction (nucleation centre) increases the cooling rate gradually decreases and austenite starts solidfying according to the following reaction :

LAE g + M6C

Starting from a segregation free area the amount of carbide precipiradon will gradually increase and the

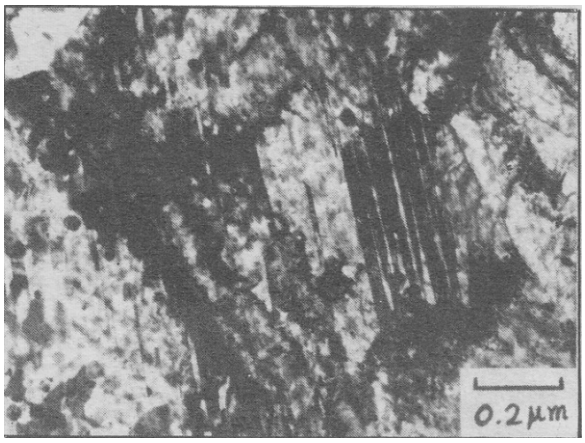

Fig.4 Transmission electron micrograph having twined martensite.

austenite will be less and less superstaturated as the cooling rate decreases with the increase in distance from the nqclea: tion site. With thc lower supersaturation the M temperanre of austenite increases (above room temperature) ?esulting transformation to martensite. The austenite which solidifies without precipitation or only with a few precipitates along cell boundaries is highly supersaturated with the alloying elements and has M, temperature below room temperature. So transformation to martensite does not take place. Partitionless growth of d-ferrite is very difficult to achieve (7), but where it does occur the modulated structure within the matrix may arise from clustering of carbon atoms on {100} d-planes (8).

CONCLUSION

1. in rapid solidification of Tl high speed steel nucleation in the electron transparent areas occurs at the points of contact of the melt with the substrate and solidification takes place in the plane of the splat/substrate interface.

2. The different types of microstructures observed are related to the distance from the point of contact of the melt with the substrate as follows : a. At the point of contact d-fenite nucleates and grows in the plane of the splat with segregation of carbide at interdendritic boundaries. If d-fenite forms as pafiitionless due to extremely high cooling rates it decomposes spinodally at room temperature. b. Austenite nuclcates on ferrite and grows initially as partitionless. As the distance from the nucleation site increases it breaks down into cellular structure with fine precipitates of carbide at cellular boundaries. c. Further away from the contact point (nucleation site) coarse precipitates of carbide are formed and austenite transforms to martensite at room temperature due to less supersatural-ion.

ACKNOWLEDGEMENTS

M. N. H. is gratcful to the ACU, U. K. for a commonwealth scholarship and to the BIIET authority for granting study leare over the period in which this research was done. The authors also wish to

thank Dr. J. A. Whiteman for his interest and help in the electron microscopy.

REFERENCES

- *1. H. Jones, Rep. Progr. Phys., 36 (1973)1425.*
- *2. J. V. Wood and LR.Sare, Proc. 2nd. Int. Conf. on Rapidly Quenched Metals, M. L T. press, Cambridge, Massachusetts, (I97 6) &7 .*
- *3. I',! 53. J. V. Wood and I. R. Sare, Metall. Trans., 6A (1975)*
- *4. I. R. Sare and R. W. K. Iloneycombe, J. Marer. Sci., i3 (1978), 1991.*
- *5. (1984).*
- *6. M. Nasrul Haque, Ph. D. Thesis, Univ. of Sheffield, I.R.Sare andR.W.K.Honeycombe,J.MetalSci., t3 (1979).269.*
- *7. M. Nasrul Haque and D. H. Kirkwood, Int. J. of Rapid Solidification, 2 (\956) 125.*
- *8. R. A. Johnson, Acra Met., 15 (tg6i.), L3.*

IMPACT AND COLLAPSIBLE STRENGTH OF BORAK VARIETY OF BAMBOO

Wazed Ali*,M. Hossain*,M. Fazli llahi*t

*** Formerly Postgraduate Sfirdents, ITS Deparunent,ICTVTR, GPO Box 3003, Ramna Onah, nangladsslr MCE DepartmenE ICTVTR, GPO Box 3003, Ramna, Dhaka.

ABSTRACT

Bamboo is being widely used as a material of construction and also for furniture, specially in the rural areas of Bangladesh. The design can be safe and economical when data on the mechanical properties areknown. One of the important variety of bamboo, Borak is widely used in Bangladesh. In this study the impact and collapsible srength of Borak have been determined and presented.

INTRODUCTION

The industrial development gives rise to demands of more appropriate properties of materials.These properties are becoming more diverse and severe. One very common indigenous material used in Bangladesh for mechanical and civil structure is bamboo. Some data is available in the literature [1991] and more experimental data are needed for proper use of this widely used material of construction. The mechanical properties which are of importance include tensile and' compressive strengths, impact strength, collapsible stength, torsional strength etc. In many structural uses like homes, furnitlre, bridges strength etc., the impact and collapsible strength are vital. One study (1992) shows that out of a total annual consumption of about 11,000 tons of bamboo and wood approximately 20Vo is bamboo used for rural fuel and 20Vo is bamboo used for rural construction and furnirure and0.57o is bamboo used in paper and pulp industry. In this present study quantitative values have been determined. For the presellt investigation only borak bamboo has been used which is a very common variety used for many applications.

NOMENCI-ATURE

F	= Force per unit contact length
Fu	= Maximum force per unit contact length .
L,b,t	= Length, width, ttrickness of specimen
d,di	= External and internal diameters of specimen
r	= Mean radius of specimen

Δ_y	=	Measured change in diameter i.e. deflection
P	=	Percent deflection ($\Delta y/d_i$) x 100
P_u	=	Percent deflection at maximum force
B.S.	=	Bamboo Stiffness ($=F/\Delta_y$)
S.F.	=	Stiffness Factor ($= 0.149\ Fr^3/\Delta_y$)
S.D.	=	Standard Deviation.

EXPEzuMENT

I) Impact Test: The Borak bamboo selected was grown in Barobari area of Gazipur district near the test site. The length of the piece brought at the test site was l2m. The outer diameter at bo$om section was 88.9 mm, at the middle section was76.2 mm and u the lop was mm. The thickness at the boEom was 19 mm. After drying for 7 days it was split up in four pieces along the length and dried for another Z days before preparing the specimen having the shape (Figure l) according to ASTM D256.The specimen length was along the longitudinal direction of the bamboo. For the Charpy and Izod tests, Brooks T 3U pendulum type of impact testing machine was used" The minimum graduation of the scale of the machine was 2 J. For the Charpy test the angle of drop was l40o wirh a maximum impct energy of 300 J and striking velocity of 5.35 m/s. The dis[ance between the supports was 40 mm and the blow was struck on the face opposite to the notch. The effect of skin of bamboo on the strength value was checked by removing about I mm thickness of the outer cover of some specimens. Also the strength without drying some of the specimens in the frnal stage i.e. in green condition was determined

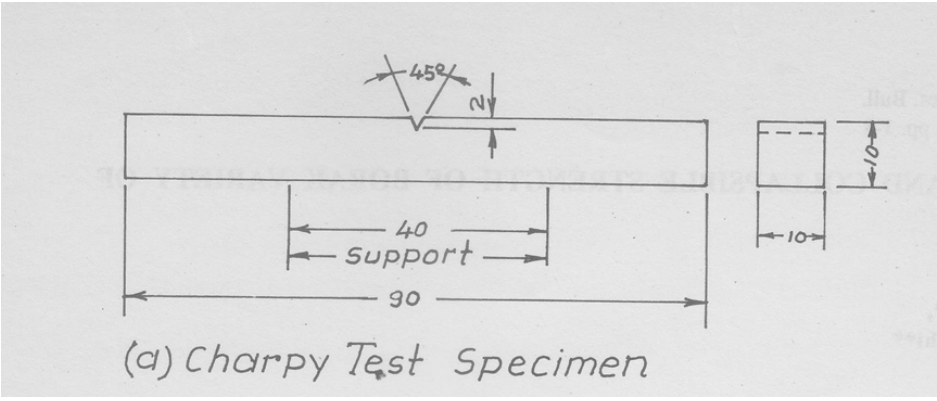

(a) Charpy Test Specimen

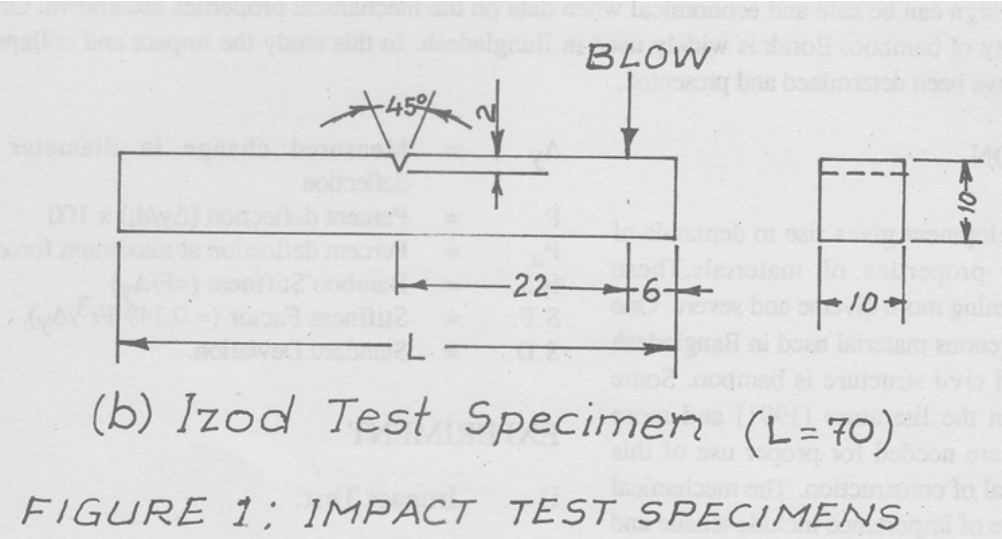

(b) Izod Test Specimen (L=70)

FIGURE 1: IMPACT TEST SPECIMENS

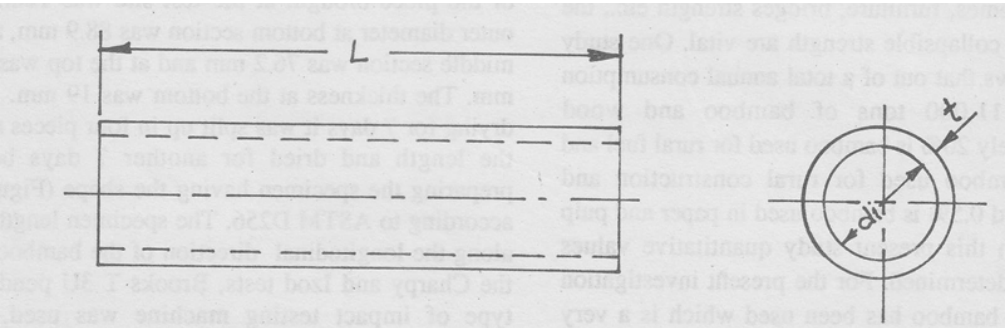

FIGURE 2: SPECIMEN FOR COLLAPSIBLE STRENGTH TEST.

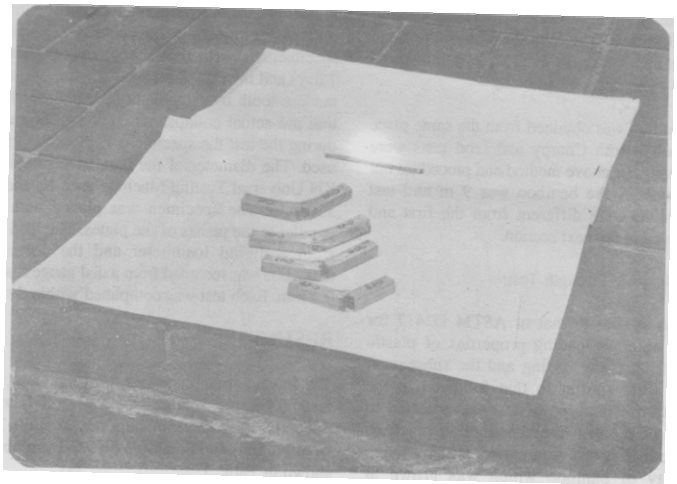

Fig. 3 : Specimens after impact tes

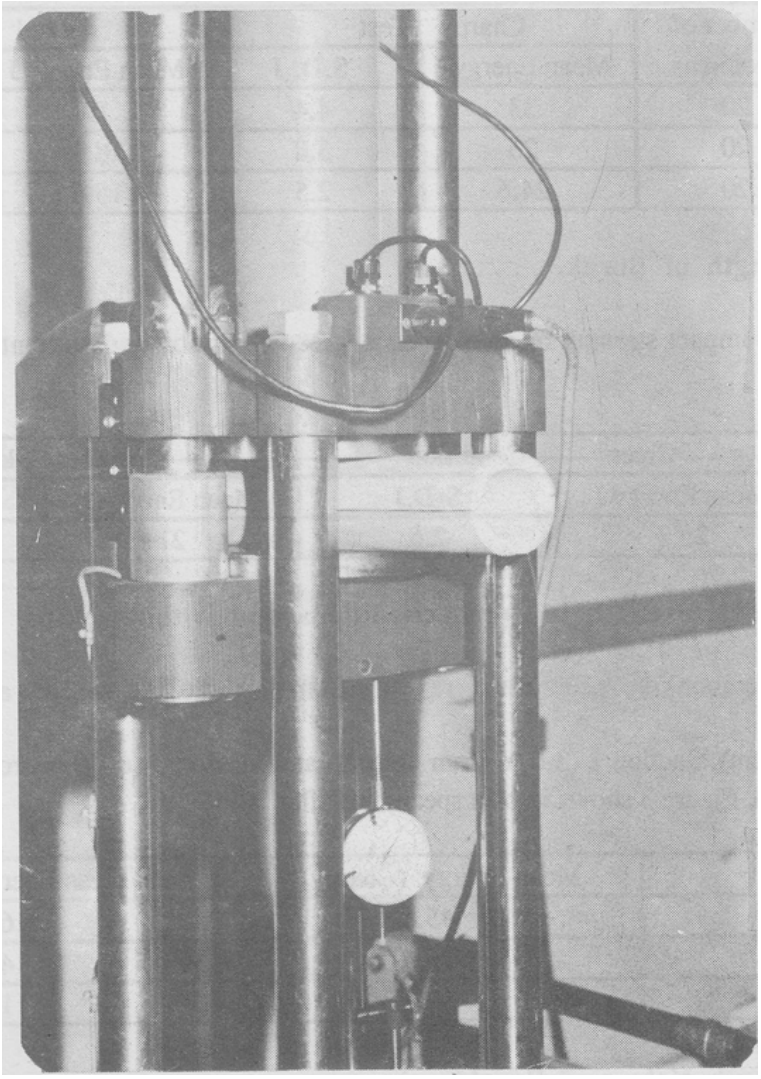

Fig.4 : Experiment in progress for determining collapsible sEength.

For the case of Izod 0est the angle ofdrop was g5o wi-tn 1 malilum impct energy of 150 J and striking velocity of 3.86 m/s. The V-norch was in tle same plane as the upper face as clamps. The blow was stnrck on the same face as fre norch.

A second bamboo was obtained from the same place as the first one. Both Charpy and lzod tests were canied out using the above method and procedure but the otal length of the bamboo *as i m and test section positions were different from the frst and details are given in the next section.

ii) Collapsible Srength Test:

This test was similar to that of ASTM D2412 fsr determining external loading properties of plastic pirys by parallel plate loading and the subsequent calculations were similar to ttrat followed in ne ASTM standard. This type of test was selected to simulate !o some extent the construction practices using bamboo. The test was carried out 6y using Borak variety of bamboo which ,uas gro*n at

Barobari area neiu the test site. The bambm was dried in sunlight for seven days before cutting the bamboo ino.pieces rejecting the knots and rn-aking rough specimens. The rough specimens were again iri"O fo, 7 {yr and then the specimens (Figure 2l wercfinally made smooth by using emery paper. It may be noted that ttre actual collapse snengtlr-will be more since during the test the specimens without the knots were used. The diameter of the parallel plates of the 100 KN Universal Testing Machine usea for the test was 150 mm. The specimen was placed with the axis parallel !o the planes of the plates. The load was read from a digital loadmeter and the corresponding deflection was recorded frrom a rrial g*g","udirrg opo 0.1 mm. Each te.st was completed "ri$in 5 minutes.

RESI.JLTS

The impact srength values from the Charpy impact tests for three sections of the first bamboo i.e. Section I (0-2 m from bot!om), Section 2 e4 m from bocom) and Section 3 (4-6 m from bottom) are shown in Table l.

Section	Number of Specimens	Charpy Test		Izod Test	
		Mean Energy J	S.D. J	Mean Energy J	S.D.J
1	20	33	4.4	19	2.4
2	20	26	3.8	18.9	1.9
3	20	24.6	2.5	15.6	2

Table 1: Impact Strength of Borak.

Table 2 shows the ch"rpy impact strength of specimens in green condition and without skin for the case of

Section	Green Condition		Without Skin	
	Mean Energy J	S.D.J	Mean Energy J	S.D. J
1	25.3	2.6	21	2.9

Table 2: charpy rmpact strength in green conditions and withouf skin.

For the case of the second bambm five specimerui were test€d from the three sections each as follows: section l(0-3 m from botom), section 2 (34 mfrom bottom) and Section 3 (6 - 9 m from botom). The test values are shown in Table 3. Figure 3 shows impact specimens after failu

Secion	Mean Energy (Charpy) J	Mean Energy (Izod) J
1	45.6	16.4
2	26.0	14.4
3	17.6	11.4

Table 3: Impact Strength 4 26.0 17.6 Values of Borak.

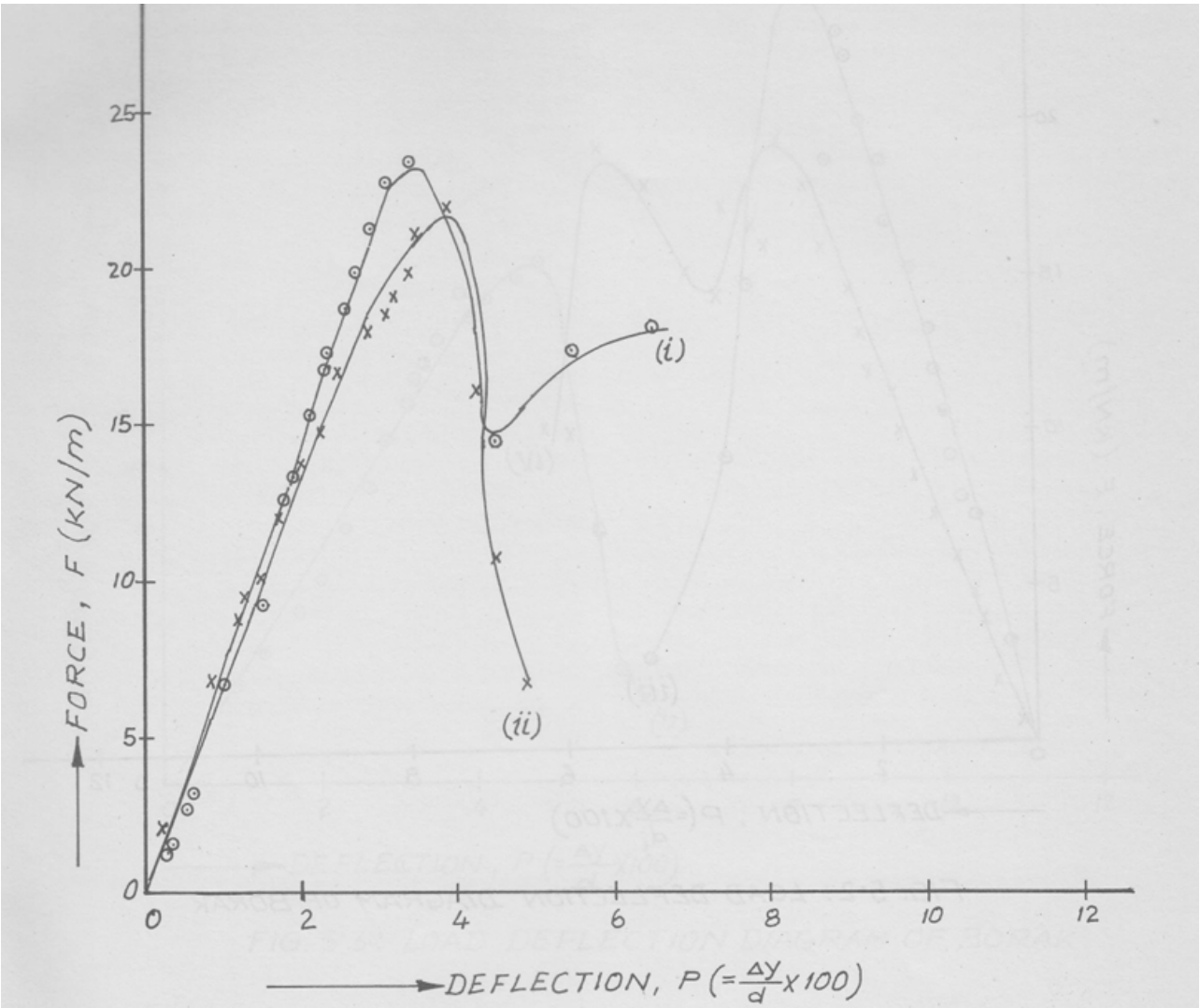

FIG. 5·1 : LOAD DEFLECTION DIAGRAM OF BORAK

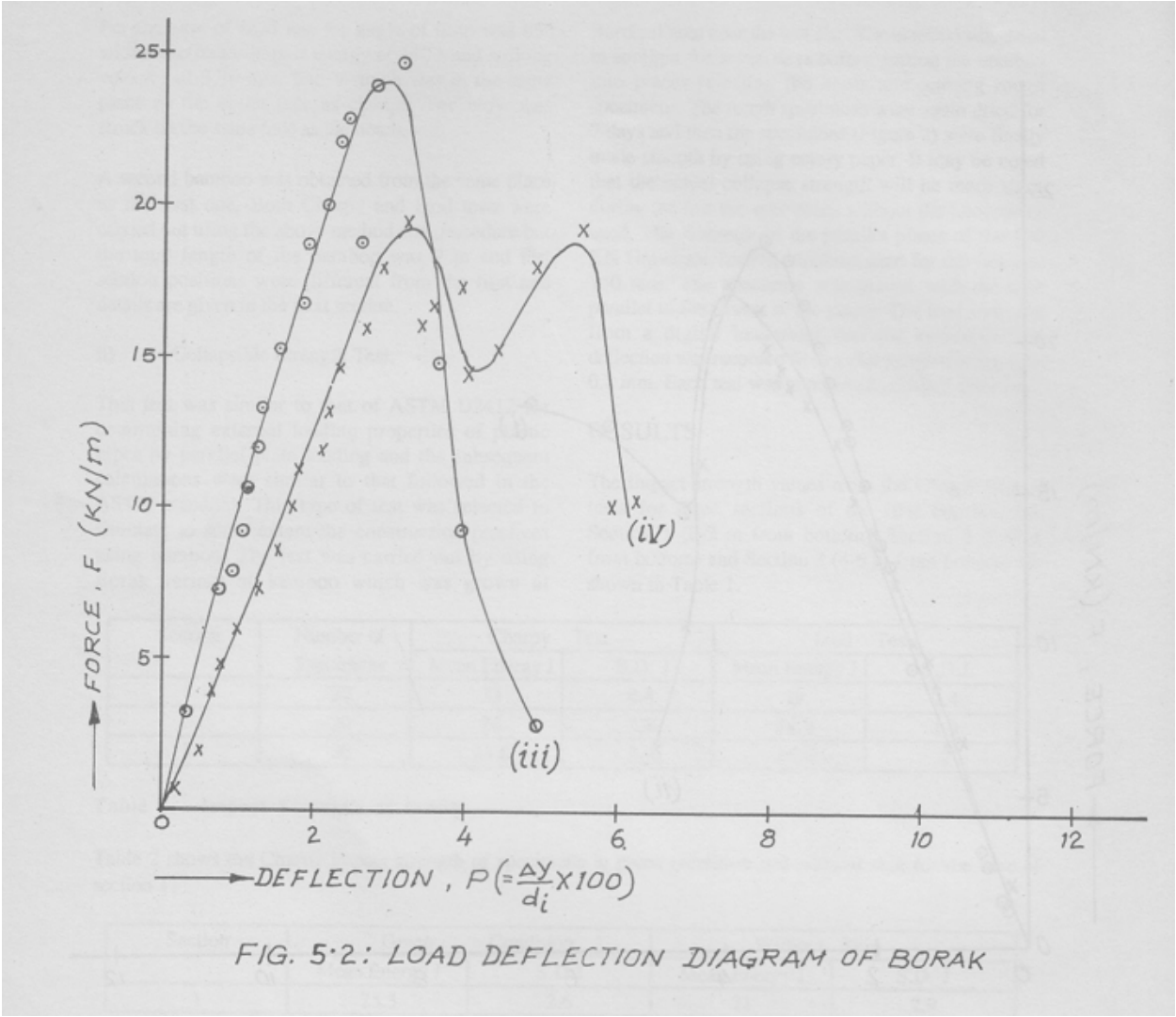

FIG. 5·2: LOAD DEFLECTION DIAGRAM OF BORAK

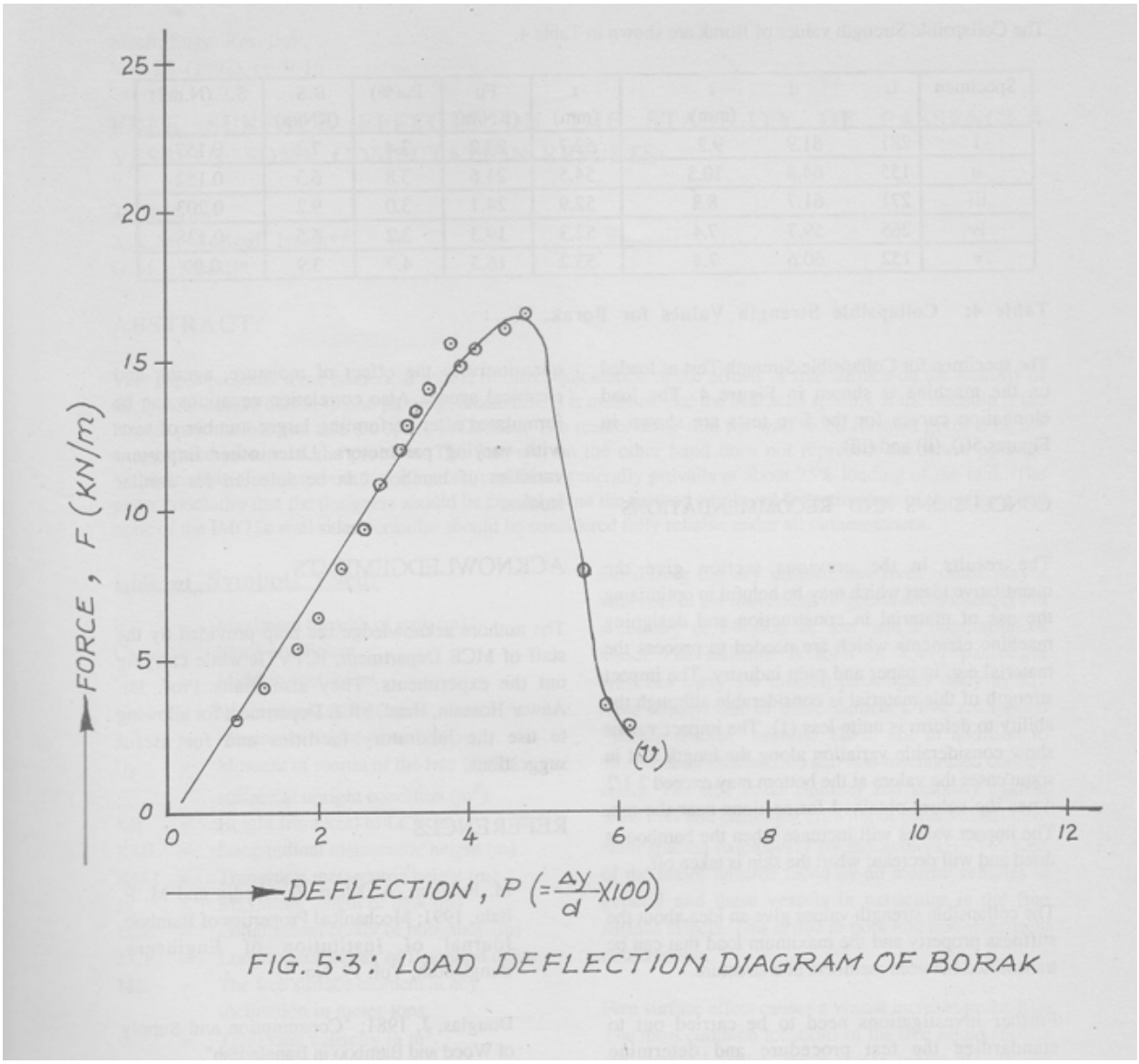

FIG. 5·3: LOAD DEFLECTION DIAGRAM OF BORAK

The Collapsible Strength values of Borak are shown in Table 4.

Specimen	L	d	t (mm)	r (mm)	Fu (KN/m)	Pu(%)	B.S. (KN/m)	S.F.(N.m2)
i	281	61.9	9.2	52.7	23.2	3.4	7.2	0.157
ii	155	64.8	10.3	54.5	21.6	3.8	6.3	0.152
iii	271	61.7	8.8	52.9	24.1	3.0	9.2	0.203
iv	265	59.7	7.4	52.3	19.3	3.2	6.5	0.138
v	152	60.6	7.4	53.2	16.5	4.7	3.9	0.09

Table 4: Collapsible Strength Values for Borak.

The specimen for Collapsible Strengrh Test as loaded on the machine is shown in Figure 4. The load elongation curves for the five tests are shown in Figures 5(I), (i0 and (iii).

CONCLUSIONS AND RECOMMENDANONS

The results in the previous section give the quantitative ideas which may be helpful in optimizing the use of material in construction and designing machine elements which are needed to process the material e.g. in paper and pulp industry. The impact strength of this material is considerable alttrough the ability o deform is quite less (l). The impact values show considerable variation along the length and in some cases the values at the bottom may exc**12lf2 times the values obtained for sections near the top. The impact values will increase when the bamboo is dried and will decrease when the skin is The collapsible strength values give an idea about the stiffness property and ttre maximum load rhat can be Eansmiued between members of a structure. Further investigations need to be carried out to standardize the test procedure and quantitatively the effect of moisture, ageing chemical agents. Also correlation equations can be formulated after performing larger number of tests with varying parameters. Later other important varieties of bamboo can be selected for similar studies.

ACKNOWLEDGEMENTS

The authors acknowledge the help provided by rhe staff of MCE Department, ICTVTR while carrying out the experiments. They also thank prof. Dr. Anwar Hossain, Head, MCE Department for allowing to use the laboratory facilities and for useful suggestion's.

REFERENCES

- *M. Rahman, A. Iihan, Z. Abedin and M. F. Ilahi, l99l; Mechanical properties of Bamboo,*

- *Journal of Institution of Engineers, Bangladesh, Vol. 19, No. 3.*
- *Douglas, J, l98l; "Consumption and Supply of Wood and Bamboo in Bangladesh,'.*

Strdy of Environmentally conscious cryogenic Cooling Machining

N. R. Dhar, S. Paul and A. B. ChattoPadhYaY

Department of Industrial &

Production Engineering' B UET,.Dhaka, Bangladesh.,
Department of Mechanical E ngine er i n g, Indian I ns titute ofTechnology (IIT), Kharagpur, India

Abstract

*In machining, a cutting tool is used toremove workpiece material to precise geometry' tolerance and finish' Cutting friction significant heat which shortens tool life' Current pi..rr", use synthetic oil based cutting fluids for cooling. These huids are environmentally hazardous and disposing of them is increasingly regulated and costly. 'Metal chips generated on a machining by product are considered hazardous because of cutting huid contamination and are generally land filled' Moreover, prolonged worker contact with cutting may cause severe dermatitis. Cryogenic machining is a promising new technology *hi"f, ..onomically addresses the current processes' environmental and health concerns. This process injects liquid nitrogen (-l96oC) through a macro-nozzle at the precise locition required to cool the tool and the immediate cutting zone. Chilling the cutting tool by liquid nitrogen jets enhances tool hardness and life' dimensionaf accuracy and improves surface Cooling the chip makes it brittle and aids removal' Becaus]e nitrogln is an abundant atmospheric constituent and the quantities used are small, there is no unfavorable environmental or health impact nor coolant disposal cost and the chips are readily recycled'*

Key words: Machining, Liquid nitrogen, Cutting forces, Tool wear, Product qualitY

INTRODUCTION

Science and Technology are growing fast, particularly due to liberalization and global cost competitiveness to meet the lrowin! demand for higher productivity, product quality and^ "r.i'"ff economy. Another reiuirement in manufacturing industries has been the control of environmental pollution, which has become a greet concern-of the modern society' The pollution creat;d in manufacturing not only affects the performances and health of the workers but also the surroundings'

Performances and the service life of the engineering products of given material depends upon their dimensional and form accuracy and surface quality. The preformed blanks are generally semi-finished and fihished by machining and grinding. But improvemenr in productivity as well as precision by increasing speed and feed are restrained by development of high cutting temperature, particularly in case of strong, hard and sticky work materials, which not only reduces life of the tools but aiso causes dimensional inaccuracy and impairs the surface integrity of the products by rapid oxidation and corrosion and inducing harmful tensile residual stress and micro cracks of the surfaces and subsurfaces

[1].

Such high cutting temperatures generally tried to be reduced by application of cutting fluids in addition to proper selection of the process parameters and tools depending upon the workmaterials. But conventional application of cutting fluid is found to be almost ineffectivewhen the cutting temperature is very high due to machining and grinding at high speeds andfeeds, when the work materials are difficult to machine and grind for their high strength and high resistance [2,3). Besides that, application of conventional cutting fluids, generally oil base, causes severe environmental pollution and inconveniences. The major socioeconomic problems that due to such use of cutting fluids are [4-7] :

(I) wetting and dirtiness of the working zone

(ii) possible damage of the machine tools by corrosion and mixing of the cutting fluid into harmful gases

(iii) biological hazards to the operators from bacterial growth in the cuning fluids [8]

(iv) requirement of additional systems for local storage, pumping, filtration, recycling, recording, large spaces and disposal of the used up fluids which fuither causes soil contamination and water pollution in the vicinity.

Attempts have been made[9] to reduce or overcome such problems by conducting machining under dry condition using sophisticated toois like high performance ceramics, cubic boron nitride and diamond tools which are extremely heat and wear resistive. But their success was limited. Very recently a unique technique has been developed where cryogen is used as the coolant. Extensive research is going on in this direction. cooling by agents like liquid nitrogen provides not only desired cooling but also environment friendlinessF0,ll]. Such cryogenic cooling provides dry, neat and cool environment during machining and grinding without any disposal problems. But the industries wouid also obviously look into the techno-economic aspects even of such novel environment friendly technique for feasibility and economical viability. The present work briefly deals with the method of application of cryogenic cooling and the observations made so far on the effects of such new technique on cutting forces, tool life and product quality, which govern the overall economy in machining.

EXPERIMENTAL INVESTIGATIONS - PROCEDURE

Liquid nitrogen drawn from a self-pressurized dewar (xL-45, usA) was impinged in the form of two thin but high speed jets through a specially developed nozzle cutting zone. Two high carbon steels (C-40 steel and C-60 steel) and two alioy steels (Ni-Cr steel and lTCrNiMo6 steel) of varying strength and hardness were machined in a heavy duty center lathe (llkW: NH22 HMT, India) by P30 carbide inserts of two different geometry (SNMG 120408-26 and SNMM 120408) at different cutting veiocity (V.) and

feed (S") under both dry and cryogenic cooling condition. Oniy the C-60 steel was machined also with soluble oil to demonstrate the ineffective/detrimental roie of conventional cutting fluid application in high production machining of steels by carbides. The experimental setup is schematically shown in Figure l.

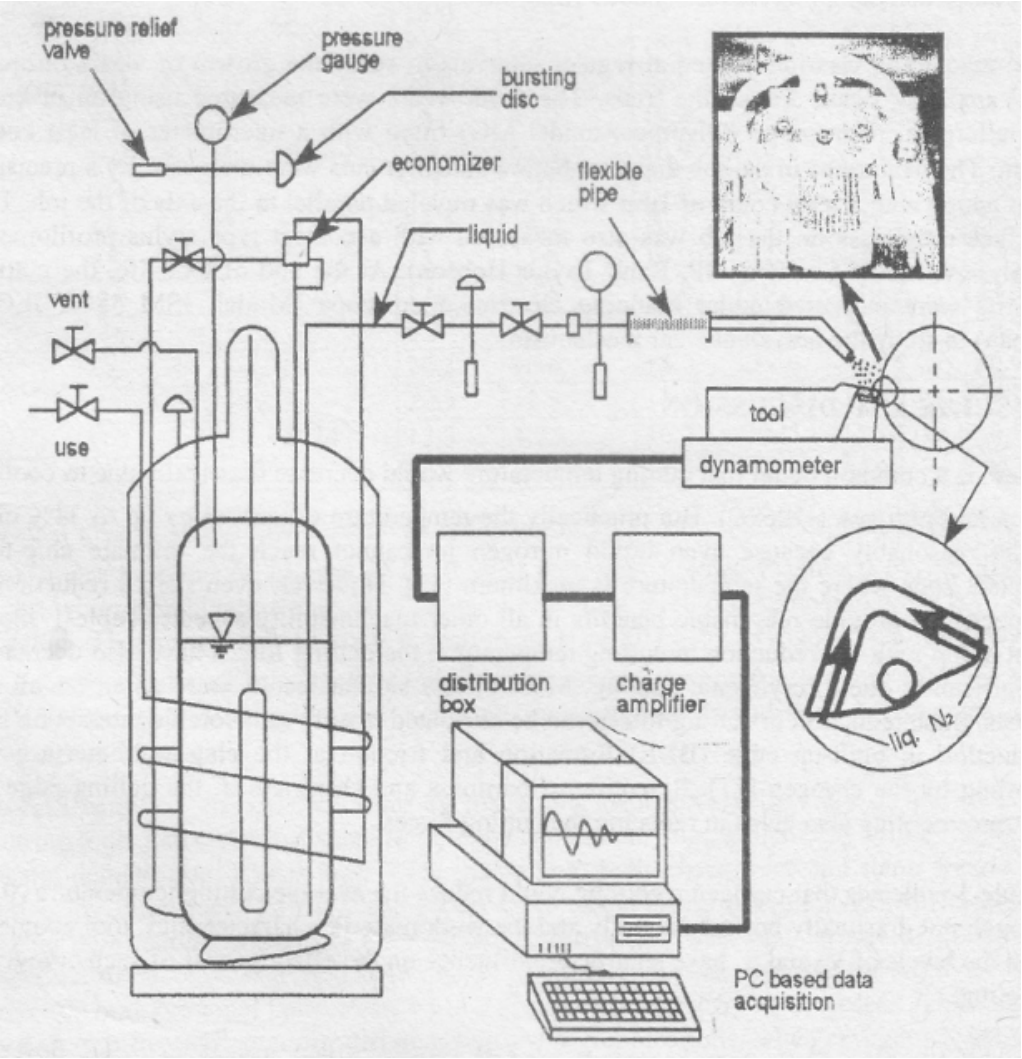

Figure 1: Schematic !aiout of experimental set-up.

Application of liquid nitrogen is expected to affect the various machinability characteristics mainly by reducing the cutting temperature. The average cutting temperature was measured by simple but reliable tool-work thermocouple technique with proper calibration. The temperature could be measured smoothly under dry machining condition but some problems like wide scatter in the temperafure readings were found to occur under cryogenic cooling. So the average cutting temperature under cryogenic cooling was evaluated using validated thermalmodeling of machining [12].

The cutting forces components, P, (tangential or main component) and P* (axial component) were

monitored by a 3-D dynamometer (ICSTLER, 3D-dynamometer, Model: 3 component dynamometer, Type: 92578; and Charge Amplifier: 5007) and recorded in a PC through a data acquisition system (Dasylab-Fullwin 95 version, PCL 818 HG l2 bit highgain multifunction DAS card and Sampling frequency 2000 Hz).

The machining was interrupted at regular intervals to study the growth of wears on main and auxiliary flanks for all the trials. The flank wears were measured using an inverted metallurgical microscope (Olympus: model MG) fitted with a micrometer of least count lpm. The deviations in the job diameter before and after cuts were measured by a precision dial gauge with a least count of I pm which was traveled parallel to the axis of the job. The surface roughness on the job was also measured with a contact type stylus profilometer (Talysurf: model Surtronic 3P, Rank Taylor Hobson). At the end of tool life, the cutting inserts were inspected under scanning electron microscope (Model: JSM 5800, JEOL, Japan) to study the prevalent wear mechanism.

RESULTS AND DISCUSSION

There is a common belief that cutting temperature would decrease drastically due to cooling by liquid nitrogen (-l96oC). But practically the temperature decreased by up to 34% only quite reasonably because even liquid nitrogen jet cannot reach the intimate chip+ool contact zone where the temperature is maximum [2]. However, even such a reduction is expected to provide reasonable benefits in all other machinability aspects. Table-l shows that along with the reduction in cutting temperature, the cutting forces have also decreased significantly due to cryogenic cooling. More or less similar results were noted for all the steels. Such reduction in cutting forces can be attributed mainly to favorable interaction like reduction in built-up edge (BUE) formation and friction at the chip-tool interface for cooling by the cryogen Il]. Retention of hardness and sharpness of the cutting edge by extreme cooling also helps in reducing the cutting forces.

Table-l indicates that cryogenic cooling could reduce the average cutting temperature (ea"s) though not drastically but substantially and the work material characteristics, tool geometry and the levels ofV. and So have significant influence on the effectiveness ofsuch cryogenic cooling.

Both the cutting force components, P2 and P* more or less decreased under different conditions with the increase in V", as usual, due to plasticization and shrinkage of the shear zone and reduced friction at the chip{ool interface and increased with increase in So simply for increase in chip load. Cryogenic cooling enabled reduce both P, and P1, though in different percentage, under different V.-So combinations and for different tool-work combinations.

Table-l Reduction in forces and eaus due to cryogenic cooling is compared to dry machining in turning C-40 steel by SNMG and SNMM inserts'

Cutting velocity, V_c m/min	Feed rate, S_o rev/min	Percentage reduction in					
		P_x	P_z	θ_{avg}	P_x	P_z	θ_{avg}
		SNMG			SNMM		
66	0.12	38.4	23.1	27.5	54.8	31.6	33.9
85		34.5	19.7	25.5	42.7	22.6	30.9
110		18.0	10.3	20.7	15.9	9.36	21.4
144		7.6	6.52	15.0	12.5	2.8	18.8
66	0.16	22.0	15.3	19.3	54.4	33.4	33.3
85		19.0	9.19	19.4	41.0	21.8	28.8
110		7.8	6.69	16.9	24.1	9.15	21.3
144		9.3	4.26	13.8	16.3	4.67	20.3
66	0.20	23.2	14.9	16.5	33.9	21.8	27.2
85		23.5	11.3	16.2	31.1	20.2	24.3
110		12.6	2.65	15.0	19.9	10.3	23.4
144		6.3	2.1	14.5	16.0	6.01	19.8
66	0.24	20.3	10.6	15.7	32.0	18.8	25.0
85		20.3	12.8	16.9	31.8	19.4	25.7
110		12.3	4.73	16.7	26.5	16.8	24.2
144		12.1	2.17	15.4	18.1	11.3	24.3

Table-1 clearly shows that percentage reduction in P" and P* due to cryogenic cooling has been more pronounced in case of C-40 steel particularly when machined by the SNMM insert which combination showed maximum recluction in cutting temperature by cryogenic cooling. The reason behind such reduction in P, and P* by cryogenic cooling may be reasonably attributed to reduction in chiptool contact length, friction and built-up edge (BUE) formation due to reduction in cutting zone temperature and favorable change in the chip-tool interaction.

Overall economy in manufacturing by machining depends significantly on the tool life. Cutting tools liki carbides generally faii by wear and only occasionally by brittle fracture or plastic deformation. Under high V.-So machining, both crater wear and flank wear occur almost by same mechanism. Most of the wear mechanisms like adhesion, diffusion and plastic deformation are temperature sensitive. Therefore, wear and its rate of growth are expected to decrease if temperature can be controlled. It was observed during the present tesis that both principal flank weor, Vs and auxiliary flank wqar, V5 decreased substantially, though in different d"gr". for different tool-work combinations, when cryogenic cooling is empioyed. Therefore, cryogenic cooling, if properly employed, would improve tool life s;gnlncantty. Fig.2 typically shows how cryogenic cooling enabled substantial reduction in tool wear unlike soluble oil which did not help at all. It is evident from Fig.3 that for vaiue of wear as 300 pm, the tool life can increase by 100 to200oh by cryogenic cooling which retarded damage and wear of the cutting edges usually caused by temperature intensive wear like adhesion and diffusion and also by

builrup edge formation.

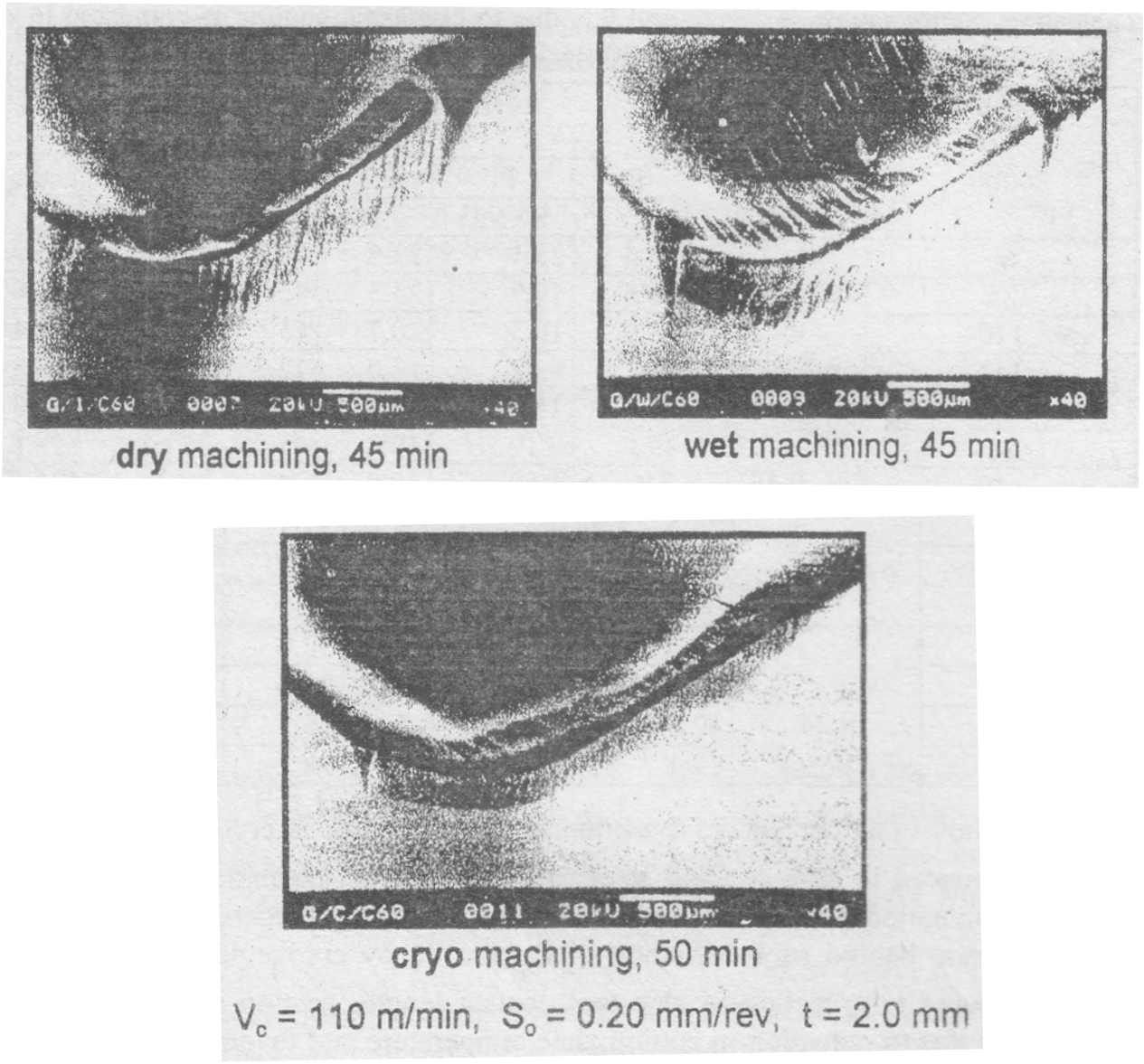

Figure 2: SEM views of the worn out SNMG insert after machining C-60 steel under dry, wet and cryogenic cooling condition.

Quality of a machined product, whi'ch governs its performance and service life depends mainly upon the material, dimensional aicuracy and surfbce integrity of the product. The heat and the cutting temperature generated iuring machiningl ii ue.y high and not controlled, may cause dimensional and form inaccuraiy due to thJrmal distortion as well as consecutive thermal expansion and cooling after machining. Bulk cooling dnd reduction of the localized cutting zone temperature byiryogenic appliJation has enabled in the present qases substantial reduction (more than 80%) in th" uu.iuiion in diameter along the length of the machined jobs. Retention of shaqpness of the auxiliary cutting edge near. the tool tip by. cryogenic application enables substantial reduction in dimensiona't Aeiiation as can be seen typically in Fig.4.

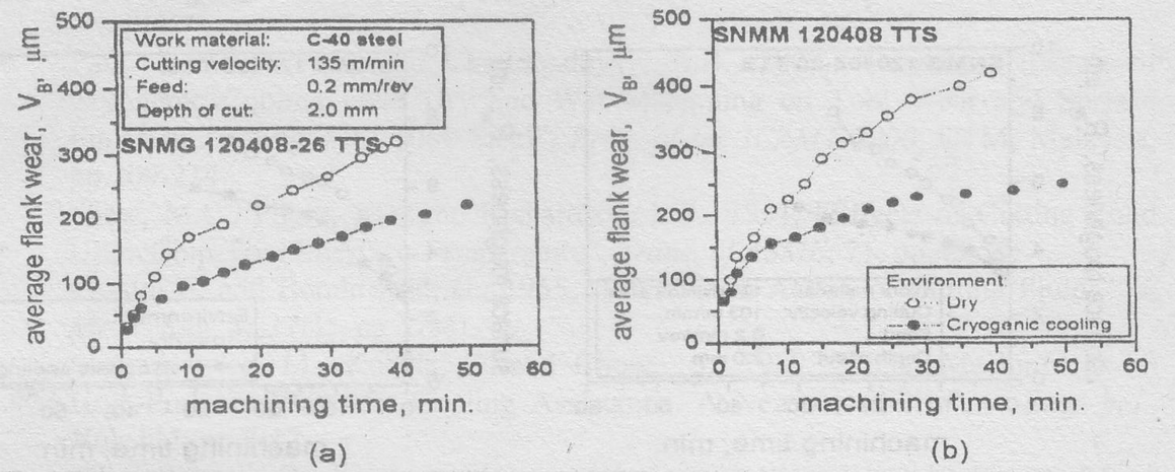

Figure 3: Growth of flank wear, V_s in (a) SNMG and (b) SNMG inserts during machining C-40 steel at V_c 135 m/min under dry and cryogenic condition.

Surface integrity generally covers both visible surface topography (roughness) and the apparently invisible aspects like residual stresses and surface and subsurface micro cracks. Surface roughness in turning is mainly caused by the feed marks and this inherent roughness depends upon the value of feed and the tool geometry, particularly the nose radius and the auxiliary cutting edge angle. The surface condition gets further degraded by the nature and extent of the wear at the nose and auxiliary flank of the cutting inserts. The improvemenr in surface finish attained by cryogenic cooling may be attributed to reduction in damage and wear of the tool nose and auxiliary flank through retention of the tool hardness and control of adhesion and diffusion. Cryogenic application also enabled significant reduction in surface roughness, as can be seen in Fig.S, quite expectedly for reduction in chipping, abrasion and notching wear at the tool tip and builfup edge

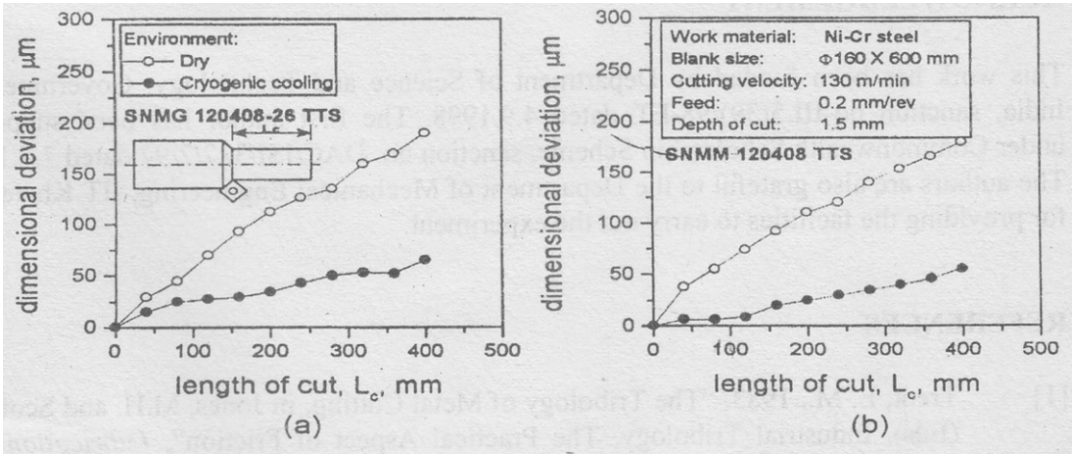

Figure 4: Dimensional derivatives observed after one full pass turning of the Ni-Cr Steel by (a) SNMG and (b) SNMG inserts under dry and cryogenic conditions.

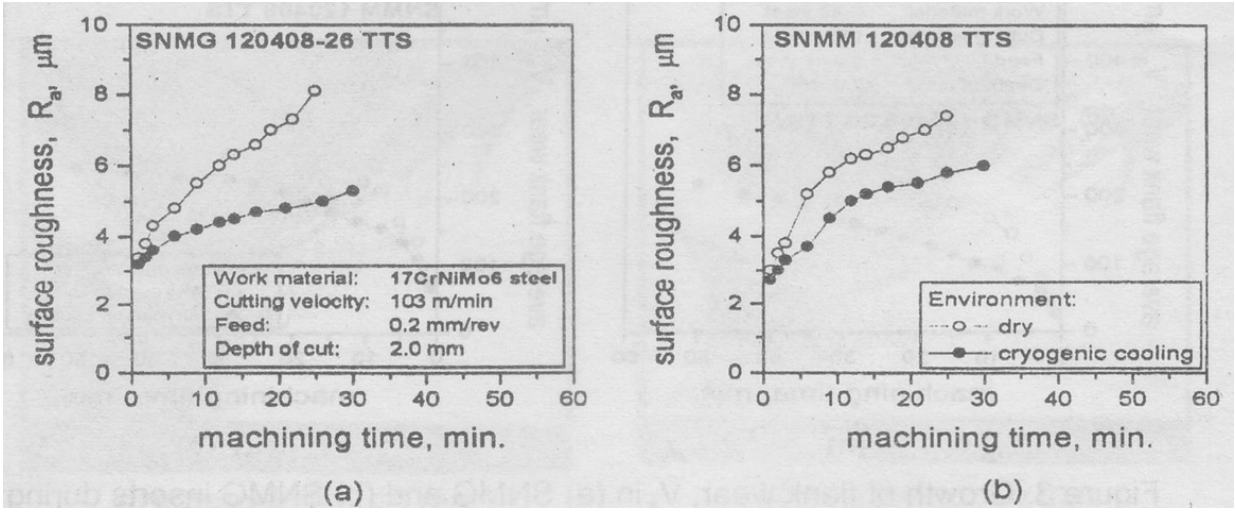

Figure 5: Surface roughness developed with progress of machining of the lTCrNiMoO Steel by (a) SNMG and (b) SNMG inserts under dry and cryogenic conditions.

CONCLUSIONS

1.Proper application ofcryogenic cooling not only provides environment friendliness but also lot of techno-economical benefits.

2. Cryogenic cooling in machining steeis by carbide inserts resulted substantial saving in energy consumption, enhancement of tool life and improvement in product quality mainly through reducing cutting forces, tool wear and friction at the chip tool interface.

3. The degree of benefits of cryogenic application in machining varies with the work tool materials and geometry and also the levels of process parameters.

ACKNOWLEDGEMENT

This rvork has been funded by Department of Science and Technology, Government of Indi'a, sanction no-III.5(39y98-ET dated 4.9.1998. The first author has been supported under Commonwealth Scholarship Scheme, sanction no. DACiISI132712197 dated7.7.1997. The authors are also grateful to the Department of Mechanical Engineering, IIT Kharagpur for providing the facilities to carry out the experiment.

REFERENCES

[1] Trent, E. M., 1983, "The Tribology of Metal Cutting, in Jones, M.H. and Scott, D. (Eds), Industrial Tribology, The Practical Aspect of Friction", Lubrication and Wear, Elsevier, Amsterdam, pp.446-47 0.

[2] Merchant, 8.M., 1958, "The Physical Chemistry of Cutting Fluid Action", Am. Chem. Soc.,

Preprint 3, No.4A, pp.179-189.

[3] Paul, S., Dhar, N.R, and Chattopadhyay, A.B., 2000, "Beneficial Effects of Cryogenic Cooling Over Dry and Wet Machining on Tool Wear and Surface Finish in Turning AISI 1060 Steel", Proc. of the ICAMT-2000, UTM, Malaysia, pp.209-214.

[4] Shaw, M.C., Pigott,. J.D. and Richardson, L.P., 1951, "Effects of Cutting Fluid Upon Chip-Tool Interface Temperature" , Trans. of ASME,7l, pp.45-56.

[5] Cassin, C. and Boothroyed, G., 1965, "Lubrication Action of Cutting Fluids",,./. Mech. Eng. Sci. 7(l), pp.67-81.

[6] Mazurkiewicz, M., Kubala, Z. and Chow, J., 1989, "Metal Machining with High-Pressure Water-Jet Cooling Assistance- A New Possibility", J. Eng. Ind., Vol, lll,pp.7-12.

[7] "High Pressure Cooling" http://www.pe.chalmers.se/projects/cool/advantages.html (2000).

[8] "Cutting Fluid Health Hazards" http//www.mfg.mtu.edu/cyberman/metal;fluids /index.html (2000).

[9] Chattopadhyay, A. 8,, Mondal, 8., Virkar, A. and Paul, S., 1992, "Development and Performance of Zirconia-Toughened Alumina Ceramic Tools", V[/ear, Vol.l56, pp.365-383.

[10] Paul, S., Banerjee, P. P. and Chattopadhyay, A. B., 1993, "Effects of Cryo Cooling in Grinding Steels", J. of Mat. Processing Tech.,Yol.37, pp.79l-800.

[11] Dhar, N. R., Paul, S. and Chattopadhyay, A,B.,2000, "A Study of Effects of Cryogenic Cooling on Chips and Cutting Forces in Turning Ni-Cr Steel", Proc. of the 1CM2000, Dhaka, Bangladesh, pp.292-300.

[12] Dhar, N. R., 2000, "Effects of Cryogenic Cooling by Liquid Nitrogen Jets on Machinability of Steels", Ph.D. Thesis, Mech. Engg. Deptt., IIT, Kharagpur, India

- *use of a direct method." International Journal of Solids and Structures 158: 90115. DOI: 10.1016/j.ijsolstr.2018.09.005.*
- *Rice, James (1968). "A Path Integral and the Approximate Analysis of Strain Concentration by Notches and Cracks." Journal of Applied Mechanics 35: 379-386. DOI: 10.1115/1.3601206.*
- *Sekiguchi, Yu, Asuka Hayashi, and Chiaki Sato (2020). "Analytical determination of adhesive layer deformation for adhesively bonded double cantilever beam test considering elasticplastic deformation." The Journal of Adhesion 96 (7): 647-664. DOI: 10.1080/00218464.2018.1489799.*
- *Sun, F., and B. R. K. Blackman (2020). "A DIC method to determine the Mode I energy release rate G, the J-integral and the traction-separation law simultaneously for adhesive joints." Engineering Fracture Mechanics 234: 107097. DOI: 10.1016/j.engfracmech.2020.107097.*

Forces on partictes nnffi.A in Turbulent FIow Through Rotating Channel

Krishnan V. pagalthivarthi and Pankaj K. Gupta
Dept. of Applied Mechanics, Indian Institute of Technology, Hauz Khas, New Delhi t l00t 6

Abstract:

*The problem of particulate flow in rotating channels serves as a usefui t.n"t*urt-for the more complex problem of. solid_fluid ,r,i*trr.r-ln rotating passag€s._ In a previous paper, the authors reported numerical simulation ol - the O.u.foping, two_ dimensional (valid for la.ge aspeci-ruiiJ'.nunn.tr;, s;teady (in the mean) and incompressiUte- canler_phase lo*. This study quantifies th. ;"i;;; *;nituo", of the most significant forces acting on u punii. carried by a turbulent flow field^I" " ."ir,i"g Jfr""".l. pressure, Coriolis, centrifugal and vii-tual mass forces are considered. particles ire treated as uniform spheres of specified diameter n A.t..rnlning ,f,. for"., acting on them. During collision with tie channel walls, they are treated as point masses. The variations of the forces- on the particie along I" p*lrl" trajectory are discussed.*

Key words: Entrained particles, nttating channel flow, forces acting on particles

INTRODUCTION

Flow of dilute solid-fluid mixtures through rotating passages is important in slurry and pneumatic transportation of solids. Two important effects of the presence of solids in such applications are: (a) the additional head loss in the passages, and (b) erosion of wetted surfaces. Both of these factors have a strong bearing on the economics of the overall operation. It is, therefore, important to understand the behavior of entrained particles and the forces acting on them in rotating passages. The straight rotating channel provides a useful benchmark for developing robust numerical methods as well as for understanding the physics of particulate flow in such situations.

A number of studies [e.g., 1-6] deal with single-phase flow in rotating channels. In a recent paper [6], the authors reported the performance of an eddy viscosity model in predicting single-phase flow through two-dimensional channels rotating in orthogonal mode (the axis of rotation is normal to the plane of the channel). A number of studies have also been conducted [e.g., 7-10] on two-phase flow through stationary channels and pipes. However, studies involving two-phase flow through rotating channels are less common. Solid-liquid flow through rotating impellers has been addressed [11, 12] using inviscid flow assumption for the carrier phase. These studies do not report a quantitative assessment of the forces acting on the particles. Moreover, viscous effects can significantly affect the base flow of the canier, particularly near the walls.

There are few studies quantifying the relative magnitudes of the forces acting on particles entrained in

flow through rotating channels. Such quantification can give valuabli insight into the head loss and erosion phenomena. The aim of this study hasleen to quantiry ihe forces on a typical particle in dilute solid-fluid flows through rotating channels.

Since the carrier-phase flow was dealt with in detail in a previous paper [6], tire present study focuses mainly on the particles. Beginningwith the equationJoimotion for a solid particle, a numerical method for tracking an individual particle is described. During collision with the walls, the particles are treated as point masses. Model coefficients o1 restitution are used in the normal and tangential directions to determine the particle velocity after impact. Impact is assumed to be instantaneous. The roughness of thi channel.walis generally have a statistical nature both in terms of the height of the surface irregularities as well as in terms of their direction with respect to the impacting particle. Some authors have attempted to include this randomness into their models for stationary passages with the concept of a virnral wall [3]. As a first approximation, this study urro1n", smooth walls, so that the direction of the normal to the wall is deterministic, not statistical. One-way coupling is assumed, 1.e., fluid flow affects the particulate flow, but not vice versa. Rotation is assumed to be in a horizontal plane, so that th'e effect of gravity may be neglected.

EQUATION OF MOTION AND NUMERJCAL METHOD

In terms of the absolute coordinate system (XYZin Figure l.) the equation of motion of a fypical particle is

$$\underbrace{\rho_S \forall \frac{d\vec{V}_p}{dt}}_{\text{Inertia}} = \underbrace{-\forall \nabla p}_{\text{Pressure}} + \underbrace{\frac{C_D A \rho}{2}\left|\vec{V}-\vec{V}_p\right|\left(\vec{V}-\vec{V}_p\right)}_{\text{Drag}} + \underbrace{\rho \forall C_v\left(\frac{d\vec{V}}{dt}-\frac{d\vec{V}_p}{dt}\right)}_{\text{Virtual Mass}}, \quad (1)$$

where ρ_S is the particle density; $\forall$ is the particle volume; t is the time; $\vec{V}_p$ and $\vec{V}$ are, respectively, the particle and fluid mean velocities with respect to ground; p is the fluid pressure; C_D is the drag coefficient; A is the project area, $\pi d_p^2/4$, of the particle of diameter d_p; ρ is the fluid density; $\hat{i}$ and $\hat{j}$ are the unit vectors in the xyz system. (coordinate system attached to rotating reference); and C_v (= 0.5 for spheres) is the virtual mass coefficient. The last term is negligible when $\rho << \rho_S$ (as in gas-solid systems).

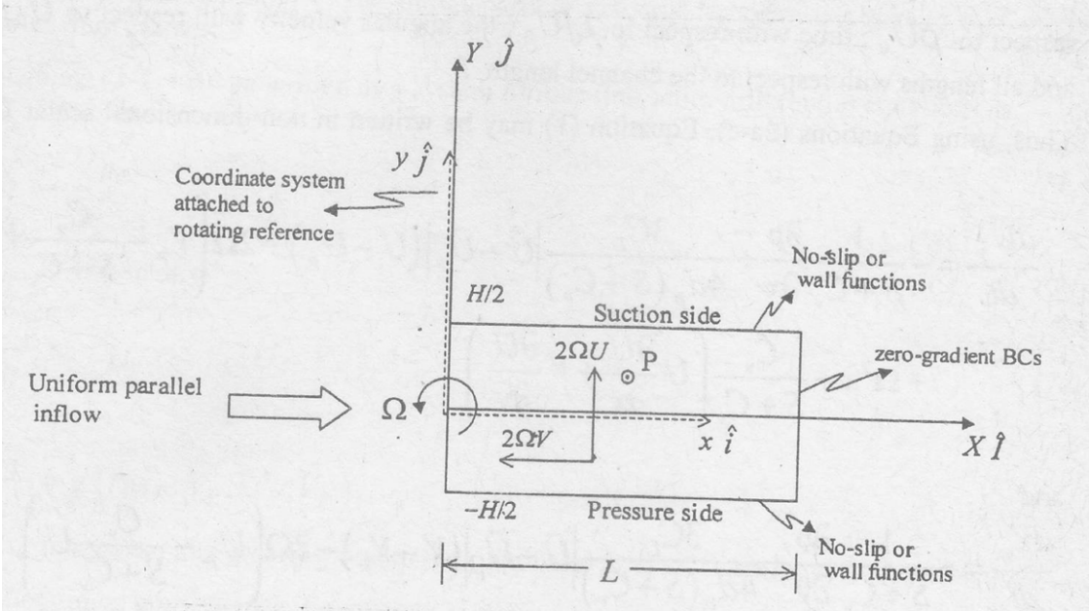

Figure 1. particle entraineO in rotating channelflow.

The relations between relative and absolute particle velocities and accelerations are

$$\vec{V}_p = \vec{U}_p + \vec{\Omega}\times\vec{r}, \text{ and } \frac{d\vec{V}_p}{dt} = \left(\frac{d\vec{U}_p}{dt}\right)_R + 2\vec{\Omega}\times\vec{U}_p + \vec{\Omega}\times\left(\vec{\Omega}\times\vec{r}\right), \quad (2a, b)$$

where $\vec{\Omega} = \Omega\hat{k}$ is the constant angular velocity of the channel. Similar expressions holdor the fluid velocity and acceleration. The subscript R denotes the rotating frame. The relative acceleration $\left(\frac{d\vec{U}}{dt}\right)_R$, the material derivative of velocity in the rotating frame, is given in terms of the local derivative and convective acceleration as

$$\left(\frac{d\vec{U}}{dt}\right)_R = \frac{\partial\vec{U}}{\partial t} + \left\{\left(\vec{U}\cdot\nabla\right)\vec{U}\right\}_R. \quad (2c)$$

Since the carrier mean flow is steady in the rotating frame of reference, $\frac{\partial\vec{U}}{\partial t} = 0$. For

convenience, the subscript R is dropped, as there is no ambiguity in its meaning in what follows.The equations are computer-coded most effectively in their non-dimensional form. Velocity is normalized with respect to the inlet uniform flow velocity, Uo; pressure with

respect to \rho U_{0}^{2} time with respect to L/U_{0} ; the angular velocity with respect to U_{0}/L and all lengths with respect to the channel length, L.Thus, using Equations (2a-c), Equation (1) may be written in non-dimensional scalar form as

$$\frac{dU_p}{dt} = -\frac{1}{S+C_v}\frac{\partial p}{\partial x} + \frac{3C_D}{4d_p(S+C_v)}\left|\vec{U}-\vec{U}_p\right|(U-U_p) + 2\Omega\left(V_p - \frac{C_v}{S+C_v}V\right) + \Omega^2 x + \frac{C_v}{S+C_v}\left(U\frac{\partial U}{\partial x} + V\frac{\partial U}{\partial y}\right) \quad (3)$$

and

$$\frac{dV_p}{dt} = -\frac{1}{S+C_v}\frac{\partial p}{\partial y} + \frac{3C_D}{4d_p(S+C_v)}\left|\vec{U}-\vec{U}_p\right|(V-V_p) - 2\Omega\left(U_p - \frac{C_v}{S+C_v}U\right) + \Omega^2 y + \frac{C_v}{S+C_v}\left(U\frac{\partial V}{\partial x} + V\frac{\partial V}{\partial y}\right), \quad (4)$$

where s is the relative density of the solid, and (Jrand vo (J and. I/) are the scarlar components of the relative velocity of the particle (fluid). The drag coefficient, c o , is calculated from the empirical correlation Ir 2]

$$C_D = \begin{cases} 0.44 & \text{when } Re_p > 1000 \\ (24/Re_p)(1+0.14Re_p^{0.7}) & \text{when } Re_p \le 1000, \end{cases}$$

where the particle Reynolds number, Re_p, is defined as

$$Re_p = \frac{\left|\vec{U}-\vec{U}_p\right| d_p}{\upsilon}.$$

Forcertaincombinationsofoperatingparameters, (Rer, Ror, plp, etc.),theparticles may slide along the channel wall. In such a case, the particle experiences a kinetic frictional resistance l4Fn,where { is the y-component (normal to the wall) of all the forces acting on the particle due to drag, pressure, coriolis, centrifugal and virhral mass forces' If the effective normal force is oli".t.o away from the wall, the particle is about to (6) separate from the substrate, and then the friction force is zero. A fourth order Runge-Kutta method [14] is employed to integrate the initial value problem represented by Equations (3) and (a). The iniiial position uio u.toriry of the particle are
specified at channel entry. The initial particle velocity is taken as equal to that of the carrier fluid at inlet. Equations (3-4) may be written as a system of four first order differential equations as

$$\frac{dx_P}{dt} = U_P, \tag{7a}$$

$$\frac{dy_P}{dt} = V_P, \tag{7b}$$

$$\frac{dU_P}{dt} = f\left(t, x_P, y_P, U_P, V_P\right), \tag{7c}$$

and

$$\frac{dV_P}{dt} = g\left(t, x_P, y_P, U_P, V_P\right), \tag{7d}$$

where functions f and g correspond to the right hand sides of Equations (3-4), respectively. For notational convenience, Equations (7a-d) may be written in vector form as

$$\underset{\sim}{W} = \underset{\sim}{q}\left(t, \underset{\sim}{W}\right), \tag{8a}$$

where

$$\underset{\sim}{W} = \left(x_P, y_P, U_P, V_P\right)^T, \tag{8b}$$

and

$$\underset{\sim}{q} = \left(U_P, V_P, f, g\right)^T. \tag{8c}$$

The prescribed initial condition is $\underset{\sim}{W}(0) = \underset{\sim}{W}_0$. The fourth order Runge-Kutta method in this study uses the following marching procedure:

$$\underset{\sim}{W}\left(t+\delta t\right) = \underset{\sim}{W}\left(t\right) + \frac{\delta t}{6}\left(k_1 + 2k_2 + 2k_3 + k_4\right) + O\left(\delta t\right)^5, \tag{9}$$

where

$$\underset{\sim}{k_1} = \underset{\sim}{q}\left(t, \underset{\sim}{W}\left(t\right)\right), \tag{10a}$$

$$\underset{\sim}{k_2} = \underset{\sim}{q}\left(t + \frac{\delta t}{2}, \underset{\sim}{W}\left(t\right) + \frac{\underset{\sim}{k_1}\delta t}{2}\right), \tag{10b}$$

$$\underset{\sim}{k_3} = \underset{\sim}{q}\left(t + \frac{\delta t}{2}, \underset{\sim}{W}\left(t\right) + \frac{\underset{\sim}{k_2}\delta t}{2}\right), \tag{10c}$$

and

$$\underset{\sim}{k_4} = \underset{\sim}{q}\left(t + \delta t, \underset{\sim}{W}\left(t\right) + \underset{\sim}{k_3}\delta t\right), \tag{10d}$$

where δt is the local time step.

Special treatment is necessary for handling particle collisions with the channel wal Particles are treated as spheres of definite diameter while solving Equations (3) and (+1 When determining the position of the particle at impact with the walls, the particles au treated as material points. In the present study, particle-wall collisions are treated instantaneous. A coefficient of restitution is introduced in both the tangential and the normal directions to compute the post-impact velocity of

the particle. The channel assumed to be unaffected in the rotating reference frame by the collisions.In Figure 2, let UPI, VPI and UP2, Vp_2 be the initial and final velocities of the particle P2 during a time step St. Let A(x,y) and B (X2,Y2) be the corresponding two positions of the particle. In the absence of the wall, the particle would trace out the path represented by the solid curve AB. The presence of the wall implies that the particle will collide before reaching point B.The point of impact C(x,y) may be determined by iteration. However, if the time step is small enough, a simple interpolation gives an accurate enough prediction of the point C and the particle velocity at the point of impact. Linear interpolation is used between A and B to locate the point C of impact. The actual time St, from A to C is also computed by interpolation.

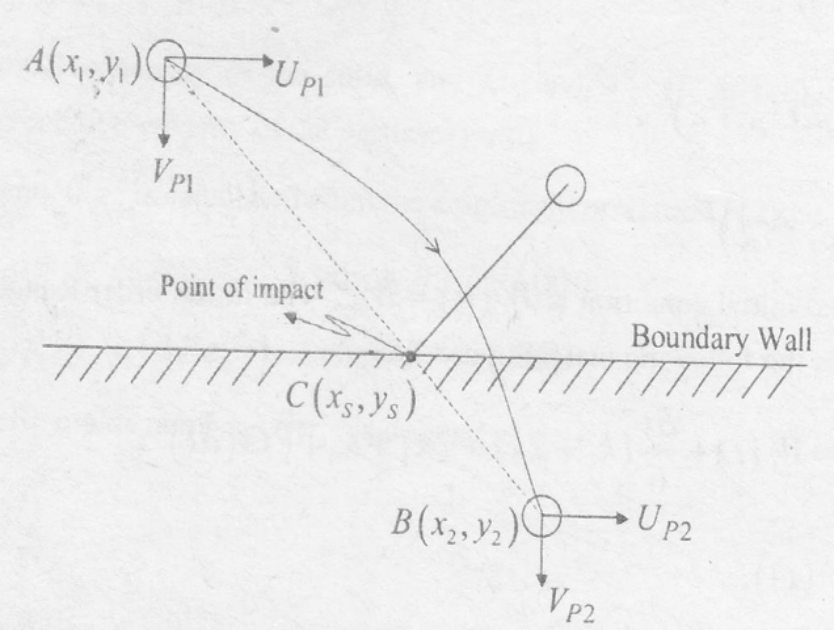

Figure 2. lnterpolation to determine point of impact.

Two more practical points are worth mentioning. First, it is possible that the post-impact normal velocity component may be quite small. In such a case, below a cut-off value, the y-component of the velocity at the wall may be set to zero, so that the particle just slides along the channel wall. Second, the center of the spherical particle can never touch the wall. In computing particle trajectory, the particle is assumed to be a material point. Thus, the wall is hypothetically shifted to the particle center, without introducing significant error. This procedure is acceptable, if the particle size is much smaller than the characteristic dimensions of the channel.

DISCUSSION OF RESULTS

The testing and validation of code by mesh refinement and comparison with published results for a

stationary channel are discussed elsewhere [6, 15]. In this section, the variations of the drag, pressure, Coriolis and centrifugal forces acting on the particle (as it moves along its trajectory in air and water) are presented. In the figures of this section, all quantities are non-dimensionalized, unless stated. For clarity, only the particle released at y = 0 (mid-height of the channel) is considered. All calculations are for the operating parameters shown in Table 1. In non- dimensional terms, the inlet velocity of both the fluid and the particle is unity.In Table 1, the quantities d, and v are the non-dimensional settling velocity of the particle in a rotating environment. These definitions are analogous to similar quantities defined for settling under the action of gravity [16]. For the rotating environment, these are defined as

$$d_p^* = d_p \left[\frac{\rho(\rho_p - \rho)(2\Omega U_0)}{\mu^2} \right]^{\frac{1}{3}} \tag{11}$$

and

$$v_{ts}^* = 1.73 \sqrt{g d_p \left(\frac{\rho_p}{\rho} - 1 \right)} \left[\frac{\rho^2}{\mu(\rho_s - \rho)(2\Omega U_0)} \right]^{\frac{1}{3}}. \tag{12}$$

It is clear from Table 1 that for the same physical diameter of $d_p = 1$ mm, the corresponding non-dimensional diameter in water is much smaller than that in air. Similarly the non-dimensional settling velocity is much larger for air than for water as the carrier. These quantities, as will be seen, characterize particle behavior to a large extent.

Table 1. Details of operating parameters

Case	Re_H	Ro_H	ρ_p (kg/m^3)	ρ (kg/m^3)	d_p (mm)	e_x	e_y	μ_k	d_p^*	v_{ts}^*
1.	11500	0.21	2700	1.23	1	1	1	0.1	99.15	17.23
2.	11500	0.21	2700	1000	1	1	1	0.1	9.105	5.22
3.	11500	0.21	1000	1.23	1	1	1	0.1	71.18	14.60

In the figures, the ordinate axis on the left-hand side of each figure shows they-coordinate of the particle trajectory. The two ordinate axes on the right-hand side of each figure show, respectively, the x-component and /-component of force (or velocity). Before getting an insight into the forces on the particle, it is useful to get an idea ofthe velocity variation. -’

Variation of Velocity of Particle

The variation of particle velocity along the length of the channel is shown in Figures 3a and 3b for air and water, respectively, as the carrier phases. The calculations correspond to Cases I and 2 of Table l.

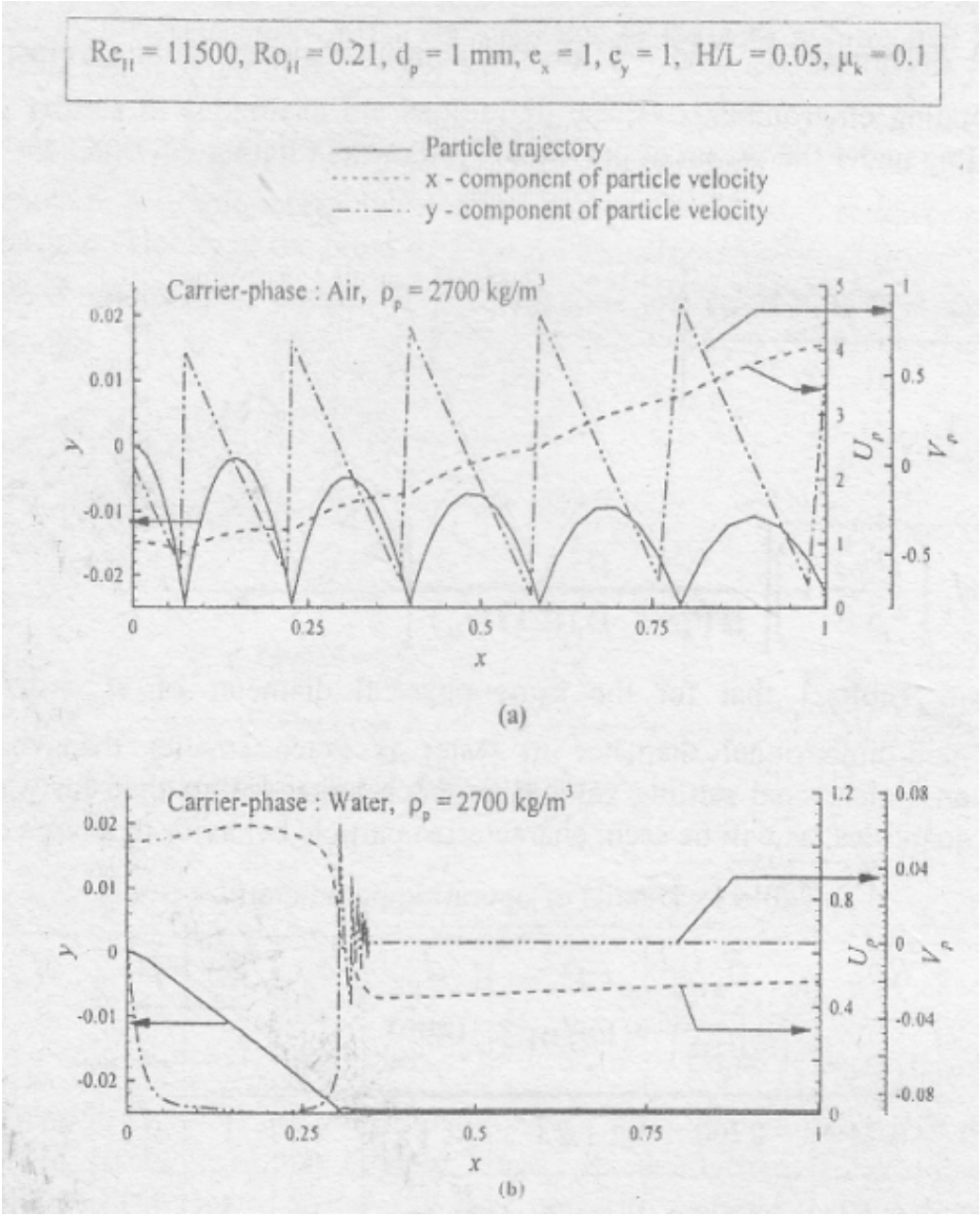

Figure 3. Variaiion of particle velocity for Cases 'l aritd Zof Table 1 with carrier phase as (a) air, and (b)water

The x-component of particle velocity. Up. increases (Figure 3a) as the particle moves along the channel length. The y-component of particle velocity. Vp. shows discontinuity at the positions of impact because Vp, changes sign at points of impact. The increase in Up, is due to the centrifugal

force, which varies as 2x. By intuition, we would expect the drag force to decrease Vp as the particle moves towards the exit. However, for air (Figure 3a), a slight increase in Vp, is seen as x increases. This corresponds to the increase in Up and hence in the Coriolis force, which varies as 220. In the absence of drag force, the increase in V, would be greater than that indicated by Figure 3a.

For water as the carrier, the variation of particle velocity, shown in Figure 3b, is seen to be completely different from that for air (Figure 3a). The drag effect in case of water is much more significant than in case of air. In Figure 3b, Up, increases initially up to x 0.125. At this stage, drag catches up and slows down the particle till it impacts with the channel pressure-side wall. After a few feeble bounces, the particle begins to slide along under the combined influence of drag and Coriolis forces. The discontinuous oscillations in Vp indicate the feeble bounces before sliding begins. After sliding begins, the centrifugal force gradually overpowers friction and drag, so that the particle begins to slowly speed up again. As the particle moves towards the pressure side, it accelerates (Vp increases) under the influence of Coriolis force. At impact, Vp reverses sign and then decelerates (since Coriolis force is now opposite to Vp).

When the particle is neutrally buoyant (p=p=1000 kg/m²), Figure 4 indicates that the particle essentially moves parallel to the channel walls, following the carrier flow. In this case, V, is nearly zero everywhere, and U, increases and reaches a plateau as the centerline velocity of the carrier fluid increases and reaches its fully developed value.

Variation of Pressure Force

In Figures Sa and Sb, the variations of the x and y components of pressure force are shown for air and water, respectively. Note from Equations (3-4) that the pressure force contains -Vp (the negative of pressure gradient). From Figures 6a, for a specified y, the pressure дp is seen to increase with x. The pressure gradient continues to increase with x and so дx does the magnitude of pressure force on the particle. Theoretically, the pressure gradient in

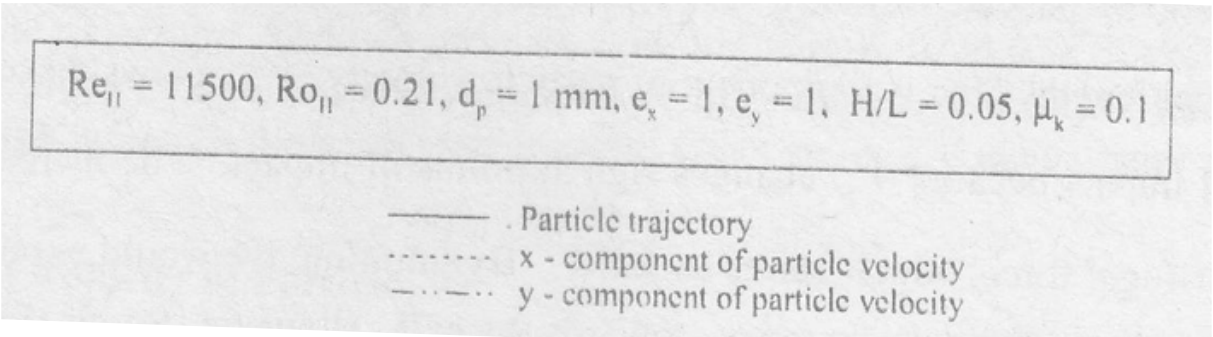

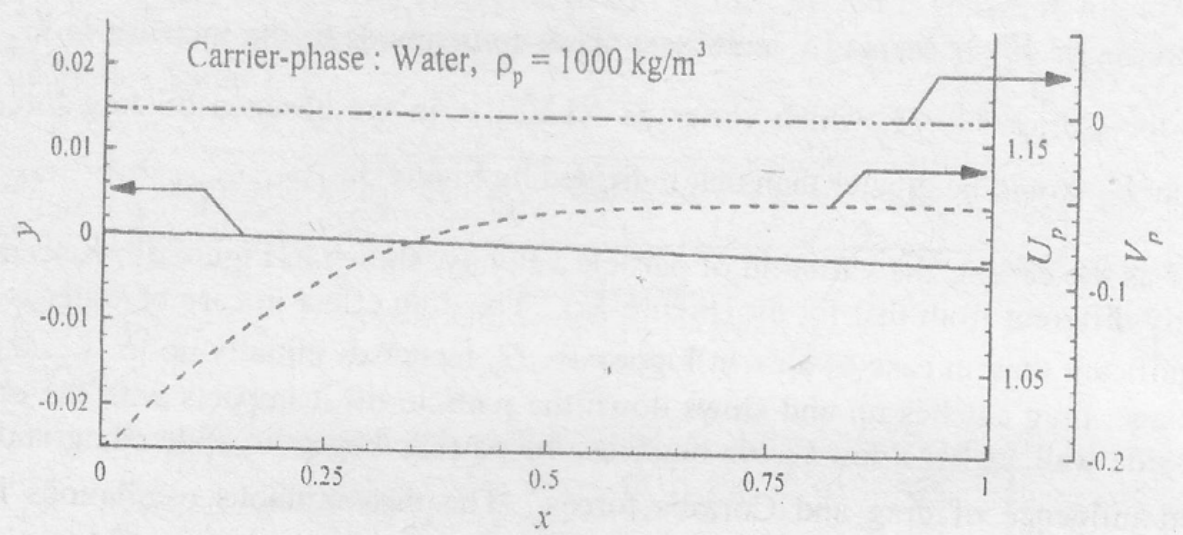

Figure 4. Variation of particle velocity for neutrally buoyant particle ($\rho_p = 1000$kg/m^3) with water as carrier-phase.

't'direction should vary as fl Ω2x (Figure 6a). This is reflected as a linear increase in thr: magnitude of the pressurei force, pf,, inFigures 5a and 5b.

The pressure force, pf y, in the y-direction varies in a somewhat complex manner. Right a

and in the vicinity of the pressure-side wall, the pressure gradient ($2\Omega U$) is nearly zero because of no-slip. Away from the wall, pressure varies linearly with y as shown in Figure 6b, *i.e.*, the pressure gradient, $\frac{\partial p}{\partial y}$ is a negative constant away from the wall. Thus, for a particle released at $y = 0$, as the particle moves towards the channel base (pressure side), initially, the pressure force pf_y, is roughly constant. As the particle approaches the wall, the *magnitude* of pressure gradient suddenly drops, and so does the pressure force. After the particle impacts and moves away from the base, the pressure force again rises suddenly. In case of air (Figure 5a), the particle reaches a substantial peak into the mainstream of the flow, *i.e.*, it reaches the constant pressure force zone after impact. Thus, pf_y remains nearly constant for some part of the trajectory, and again the process is repeated along the particle trajectory.

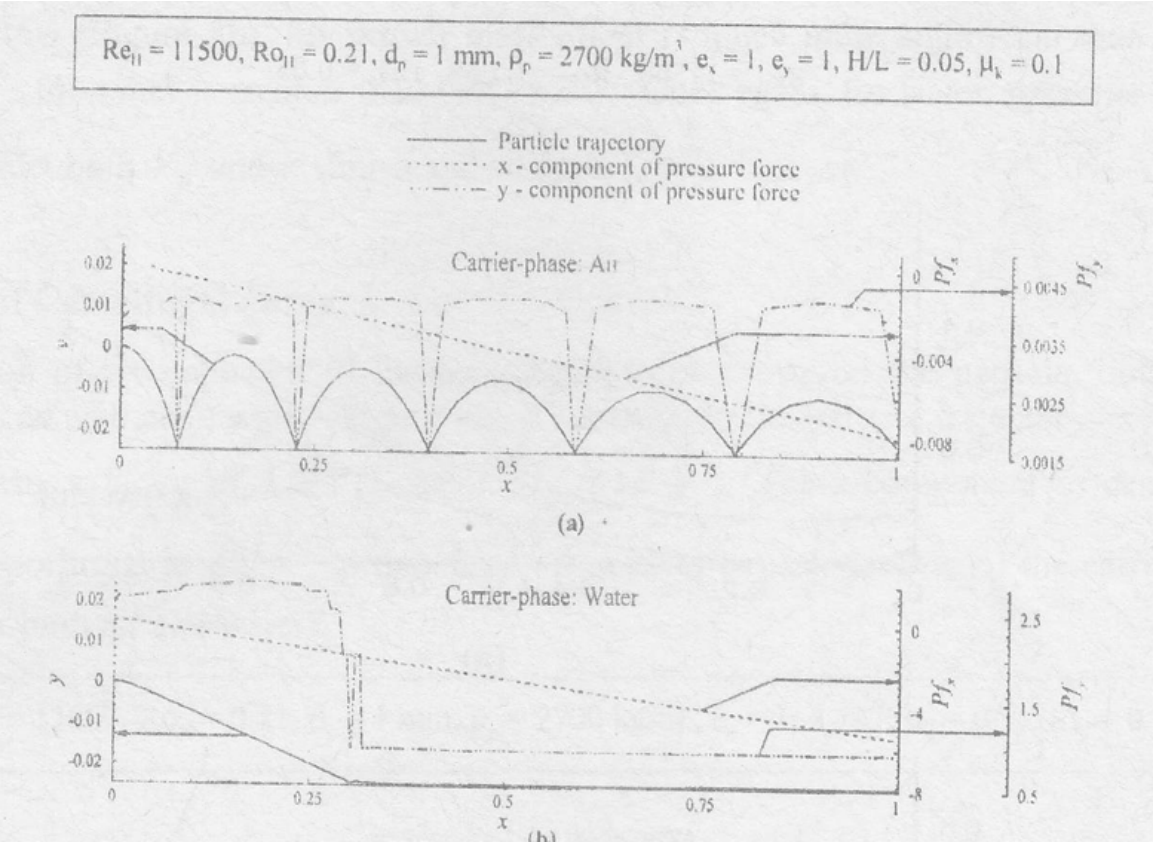

Figure 5. Variation of pressure force acting on the particle with carrier-phase as (a) air, and (b) water.

In the case of water (Figure 5b), the particle does not move sufficiently far from the wall after the bounce. Thus, pf_y does not quite increase as much as in the case of air. Once the particle starts sliding, pf_y also attains a constant value.

Variation of Drag Force

Variations for drag forces, Df_x and Df_y are shown in Figures 7a and 7b, respectively, for air and water. As noted with reference to Figure 3a, U_p tends to increase with x. Thus, the slip velocity ($U_p - U$) increases and so does the particle Reynolds number. The drag force, which is proportional to ($U - U_p$) (Equation 3), increases in magnitude (note the negative sign). Discontinuous sign reversals are seen in Df_y corresponding to the impact locations, where V_p changes sign. Furthermore, as the particle traverses along its trajectory, V_p decreases in magnitude, which results in a decrease in $|V_p - V|$, and hence a decrease in Re_p with increasing x. Thus in an overall sense $|Df_y|$ increases with x. For the case of water, Figure 7b, the particle begins to slide for $x > 0.3$ and the drag force $|Df_y|$ is zero. Note that the magnitude of drag force in air is much smaller than that in water.

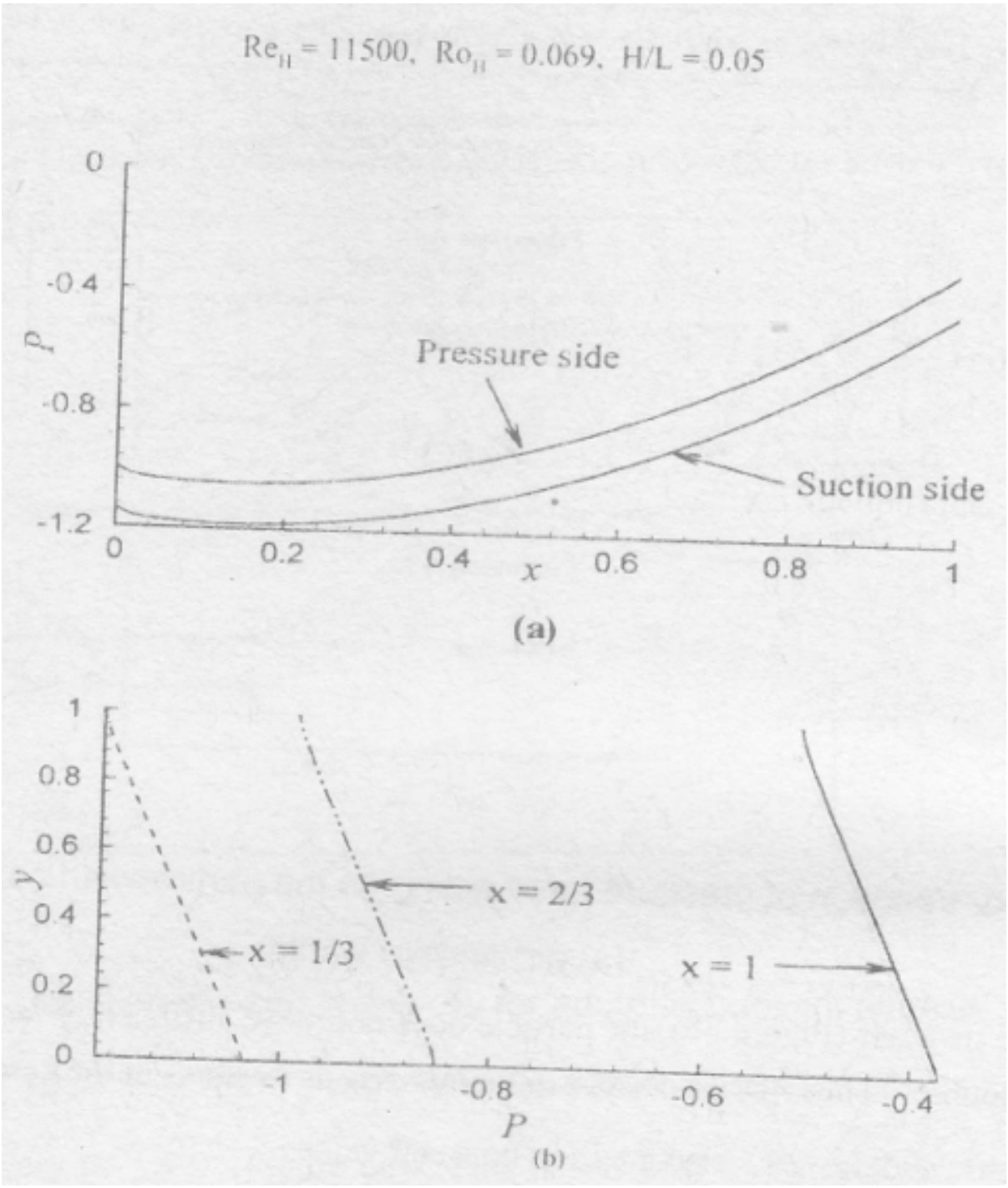

Figure 6. Variation of pressure (a) along the channel length, and (b) across the channel height.

Variation of Coriolis Force

The variation of Coriolis force acting on the particles in airflow is shown in Figure 8a. Including the effect of virtual mass, the non-dimensionalized x-component of Coriolis force is, $2\Omega\left(V_p - \frac{C_v}{S+C_v}V\right)$ and its y-component is $-2\Omega\left(U_p - \frac{C_v}{S+C_v}U\right)$. The discontinuities in Cof_x at the points of impact match with those in V_p. The y-component of Coriolis force increases in magnitude along the channel length because the term, $+2\Omega\left(U_p - \frac{C_v}{S+C_v}U\right)$, increases along the channel length.

For water flow (Figure 8b). the virtual mass effect is much more significant than for air. Thus, Cof , for water is smaller than that for air. Once again, for water, once the pafiicle begins to slide, both Vo and Zvanish and so does Cof,

Variation of Centrifugal Force

The variation of y-component of the centrifugal force acting on the particle, both in air (Figure 9a), as well as in water (Figure 9b) is identical to the particle trajectory except that it is scaled by a factor of d22. (Note: geft=tl'y.) The x-component of centrifugal force is proportional to f,l2x , so that Cef, is seen to be independent of the carrier (it is identical for both air and water).

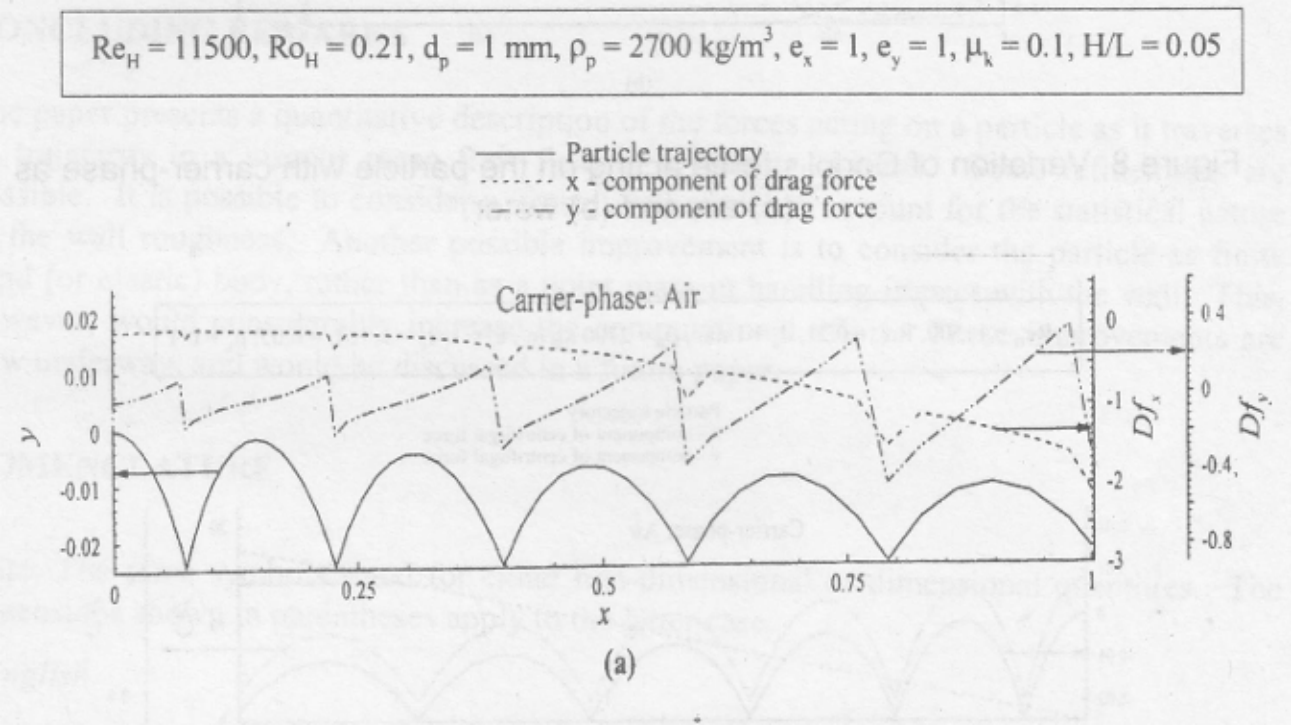

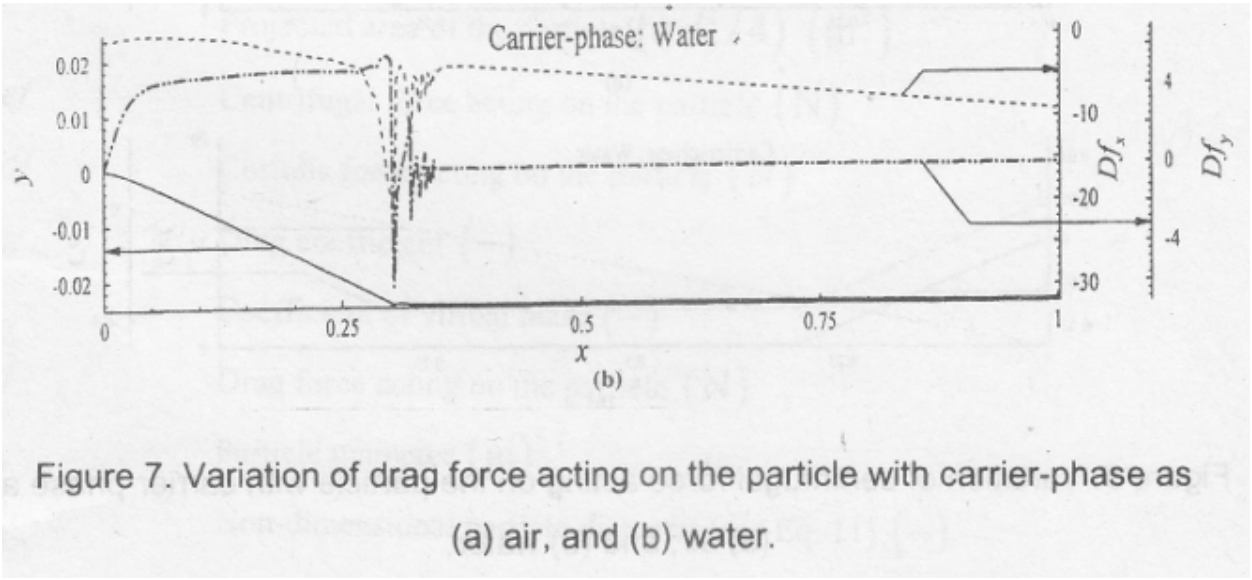

Figure 7. Variation of drag force acting on the particle with carrier-phase as (a) air, and (b) water.

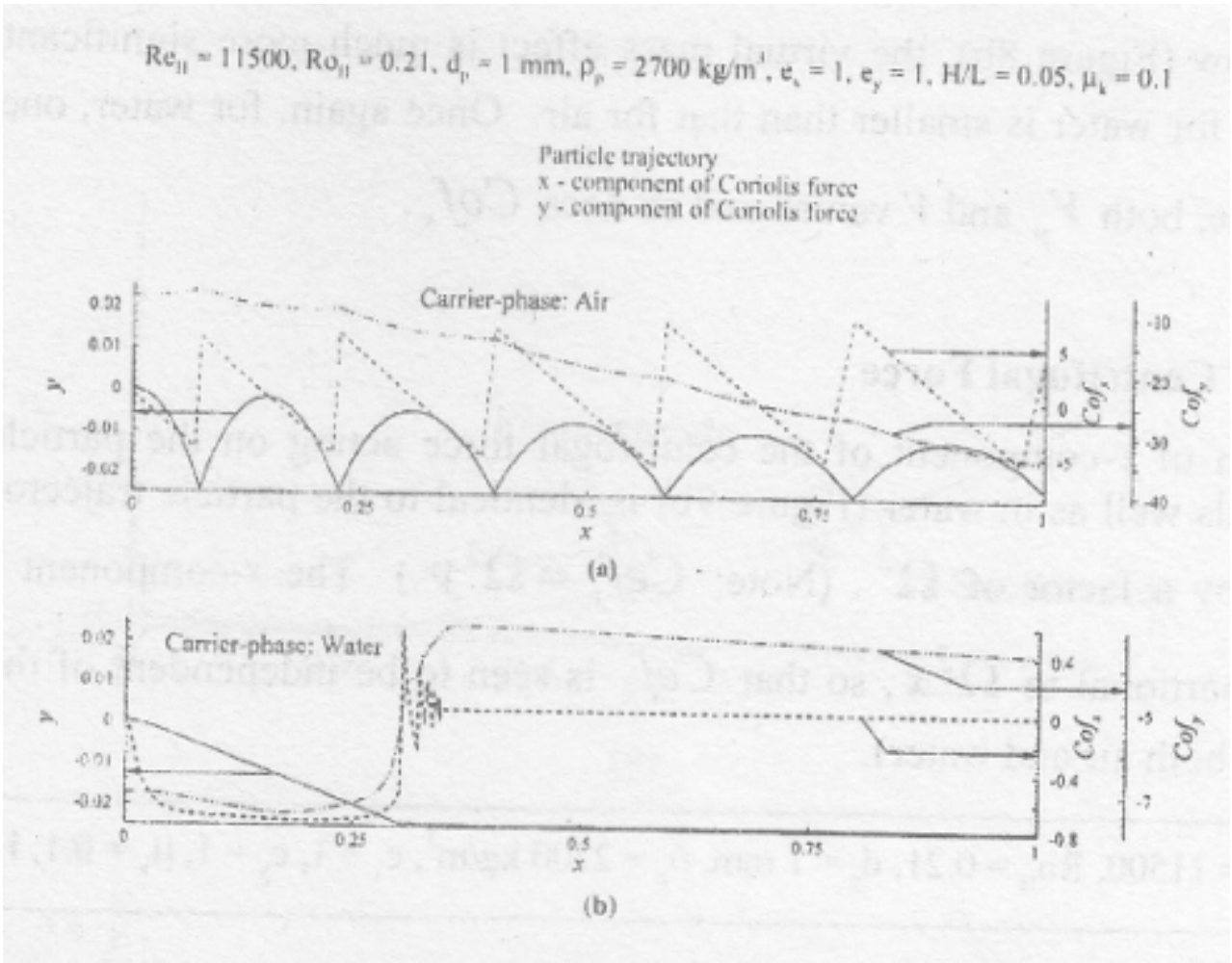

Figure 8. Variation of coriol,s force acting on the particle with carrier-phase as; (a) air, and (b) water

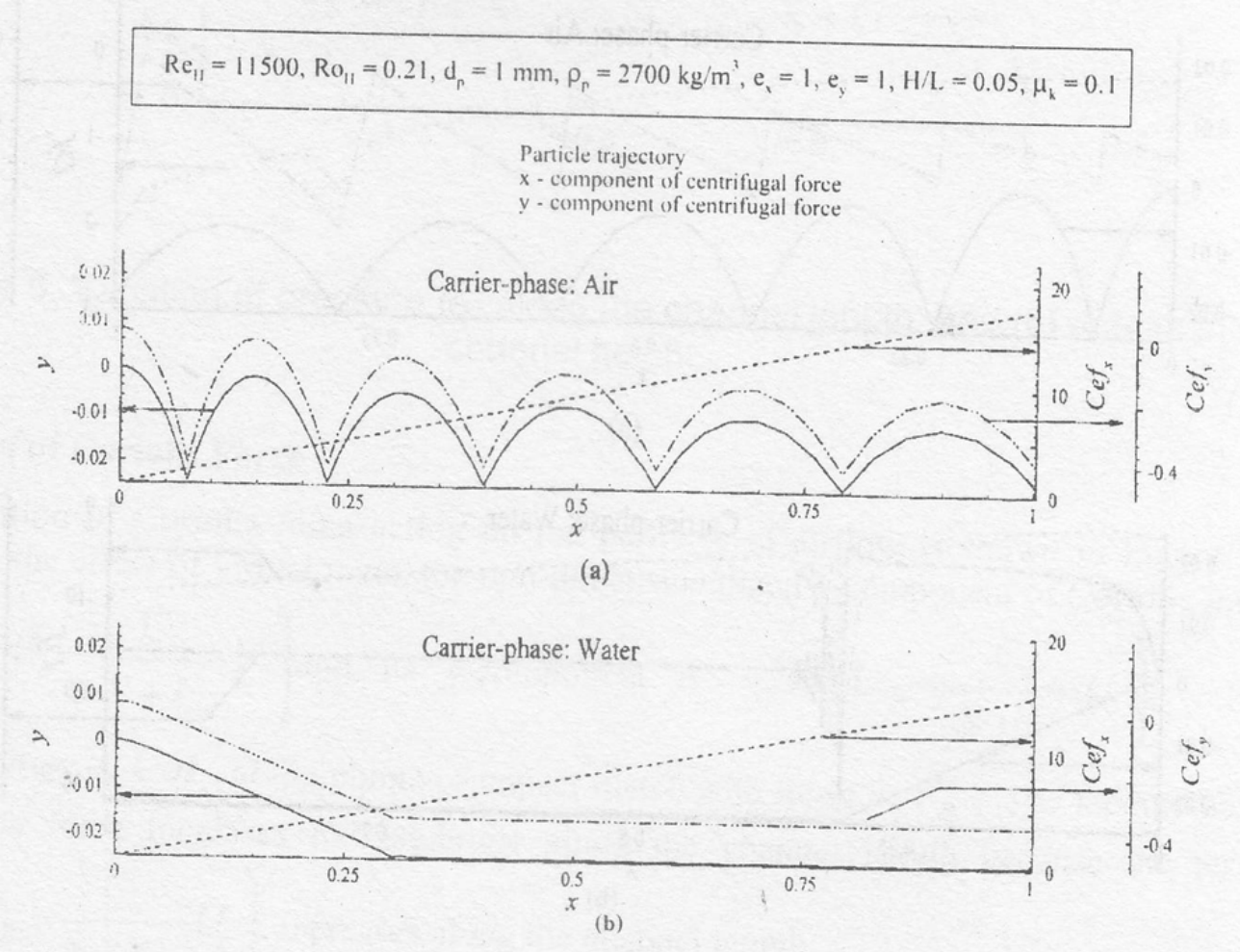

Figure 9' Variation of centrifugal force acting on the particle with carrier-phase as (a) air, and (b) water

In summary, it is seen_ that the Coriolis, drag and centrifugal forces on the particle are predominant in air' In particular, the Coriolis force grJu,ly-a.ilrmines the particle trajectory' In.water, pressure forces are also comparable to the other forces. From the trajectories, it is that with water as the canier, the particles tend to ,iia. utong the channel, with hardly a few feeble bounces. In addition, iince the coriolis force oi trr" purti.l. increases with .r, the sliding_wear rate along the pressure ,iae of the channel may be expected to increase with x' This is actually our"ruia in the coriolis wear tester 1tzi. in sharp contrast, with airas_the carrier, hardly any sliding is seen. fnur, ti,. wear rnechanism in the case of air is likely to be_governei by partici-e impact. In practice, the ,t:l7lt wear t'ester.may be modified for pneurnatic tests *itrr parti"rJr in order to measure lmpact wear coefflcrents.

CONCLUDING REMARKS

The paperpresents a quantitative description of the forces acting on a par-ticle as it traverses its trajectory in a viscous mean flow held in a rotating chaniel. dome refinements are possible' It is possible to consider a virtual wall model io u..ouni r*-ilt. of the wall roughness' Another possible irnprovernent is to consider the particle as finite rigid (or elastic) body, rather than as a point rnass in handring i*p;;; with the walr. This, however, would considerably increar. th, "orpurational ,rdrt. tn"re irnprovements are now underway, and would be discussed in a future paper.

NOMENCLATURE

Note: The same symbols stand for either non-dimensional or dirnensional quantities. The dimensions shown in parentheses apply to the latter case.

English

A	Projected area of the particle $\left(\pi d_p^2/4\right)$ $\left(\mathrm{m}^2\right)$
Cef	Centrifugal force acting on the particle $\left(\mathrm{N}\right)$
Cof	Coriolis force acting on the particle $\left(\mathrm{N}\right)$
C_D	Drag coefficient $\left(-\right)$
C_v	Coefficient of virtual mass $\left(-\right)$
Df	Drag force acting on the particle $\left(\mathrm{N}\right)$
d_p	Particle diameter $\left(\mathrm{m}\right)$
d_p^*	Non-dimensional particle diameter (see Eq. 11) $\left(-\right)$
F_n	y-component of all the forces acting on the particle $\left(\mathrm{N}\right)$
g	Acceleration due to gravity $\left(\mathrm{m/s^2}\right)$
H	Height of the channel $\left(\mathrm{m}\right)$
$\hat{I},\hat{J},\hat{K}$	Unit vectors in X-, Y- and Z- directions respectively
$\hat{i},\hat{j},\hat{k}$	Unit vectors in x-, y- and z- directions respectively
$\underset{\sim}{k}_1,\underset{\sim}{k}_2,\underset{\sim}{k}_3,\underset{\sim}{k}_4$	Vectors computed during Runge-Kutta steps
L	Length of the channel $\left(\mathrm{m}\right)$
O	Of the order of
p	Pressure $\left(\mathrm{N/m^2}\right)$

pf	Pressure force acting on the particle (N)
$\underset{\sim}{q}$	Vector defined in Equation (8c)
Re	Length based Reynolds number $(-)$
Re_H	Height based Reynolds number $(-)$
Re_p	Particle Reynolds number $(-)$
Ro	Rotation number $(-)$
Ro_H	Height based rotation number $(-)$
Ro_x	Rotation number based on distance x from origin $(-)$
$\vec{r}$	Position vector (m)
S	Ratio of solid density to fluid density (Eqs. 3 and 4) $(-)$
t	Time (m)
U	x-component of $\vec{U}$ $(\mathrm{m/s})$
$\vec{U}$	Fluid mean velocity vector with respect to rotating reference $(\mathrm{m/s})$
U_p	x-component of $\vec{U}_P$ $(\mathrm{m/s})$
U_p	x-component of particle velocity $(\mathrm{m/s})$
$\vec{U}_p$	Particle mean velocity vector with respect to rotating reference $(\mathrm{m/s})$
U_0	Inlet velocity $(\mathrm{m/s})$
V	y-component of $\vec{U}$ $(\mathrm{m/s})$
$\vec{V}$	Fluid mean velocity vector with respect to inertial reference $(\mathrm{m/s})$
$\vec{V}_p$	Particle mean velocity vector with respect to inertial reference $(\mathrm{m/s})$
V_p	y-component of $\vec{U}_p$ $(\mathrm{m/s})$
V_p	y-component of particle velocity $(\mathrm{m/s})$
v_{ts}^*	Non-dimensional terminal velocity of the particle $(-)$
$\underset{\sim}{W}$	Vector of particle position and velocity defined in Equation (8b)
XYZ	Coordinate system attached to inertial reference frame
xyz	Coordinate system attached to rotating reference frame
Greek	
δt	Time step in Runge-Kutta integration (s)
μ_k	Coefficient of kinetic friction $(-)$

μ	Laminar viscosity $(\mathrm{kg/m \cdot s})$
ρ	Fluid density $(\mathrm{kg/m^3})$
ρ_P or ρ_s	Particle (solid) density $(\mathrm{kg/m^3})$
υ	Laminar kinematic viscosity $(\mathrm{kg/m \cdot s})$
Ω	Angular speed $(\mathrm{rad/s})$
$\vec{\Omega}$	Angular velocity vector $(\mathrm{rad/s})$
$\forall$	Particle volume $(\mathrm{m^3})$
∇	Gradient operator

Subscripts

i, j, k	Dummy indices
P	Quantities pertaining to a particle
R	Relative
x	component in direction of *x*-axis
y	component in direction of *y*-axis

ACKNOWLEDGEMENTS

The authors are thankful to Vipin Narang for his help in preparing the manuscript.

REFERENCES

[1] Howard J.H.G., Patankar S.V. and Bordynuik R.M., 1980, "Flow Prediction in Rotating Ducts Using Coriolis-Modified Turbulence Models," ASME J. FluidsEng, Vol. 102, pp. 456-461.

[2] Younis B.A., 1993, "Prediction of Turbulent Flows in Rotating Rectangular Ducts," Transactions of the ASME FED, Vol. 115, pp. 646-652.

[3] Johnston J.P., Halleen R.M. and Lezius D.K., 1972, "Effects of Spanwise Rotation on the Structure of Two-Dimensional Fully Developed Turbulent Channel Flow,"J Fluid Mech., Vol. 56, pp. 533-557.

[4] Pagalthivarthi K.V. and Ramanathan V.R., 2001, "Finite Element Prediction of Viscous Free Surface Flow in Rotating Channel," Int. J. Num. Meth. Fluids, Accepted for Publication (MS#G00-

31).

[5] Majumdar A.K. and Spalding D.B., 1977, "Numerical Investigation of Three- Dimensional Flows in a Rotating Duct by a Partially Parabolic Procedure," ASME Paper 77-WAFE-7.

[6] Pagalthivarthi K.V. and Gupta P.K., 2001, "Performance of Eddy Viscosity Model in Rotating Channel Flow," J. Mech. Eng. Res. Dev., (communicated).

[7] Tsuji Y., Morikawa Y., Tanaka T., Nakatsukasa N. and Nakatani M., 1987, "Numerical Simulation of Gas-Solid Two-Phase Flow in a Two-Dimensional Horizontal Channel," Int. J. Multiphase Flow, Vol. 13, pp. 671-684.

[8] Nguyen A.V. and Fletcher C.A.J., 1999, "Particle Interaction with the Wall Surface in Two-Phase Gas-Solid Particle Flow," Int. J. Multiphase Flow, Vol. 25,

pp. 139-154. Roco M.C. and Shook C.A., 1983, "Modeling of Slurry Flow: The Effect of Particle Size," Canadian Journal of Chemical Engineering, Vol. 61, pp. 494-503. [9]

[10] Roco M.C. and Shook C.A., 1991, "Slurry Flow Principles," Butterworth- Heinemann Series in Chemical Engineering.

[11] Roco M.C. and Reinhardt E., 1980, "Calculation of Solid Particle Concentration in Centrifugal Impellers Using Finite Element Technique," Proc. Hydrotransport 7 Conf., BHRA, pp. 359-376.

[12] K. Minemura, T. Uchiyama, Calculation of the three-dimensional behavior of spherical solid particles entrained in a radial-flow impeller pump, Proc. Instn. Mech. Engrs. Part C: Journal of Mechanical Engineering Science 204 (1990) 159- 168.

[13] Sommerfeld M., 1992, "Modeling of Particle-Wall Collisions in Confined Gas-Particle Flows," Int. J. Multiphase Flow, Vol. 18, pp. 905-926.

[14] Carnahan B.; Luther H. A. and Wilkes J. O., 1969, "Applied Numerical Methods," John Wiley and Sons, New York.

[15] Carnahan B., Luther H. A. and Wilkes J. O., 1969, "Applied Numerical Methods," John Wiley and Sons, New York.

[16] Wilson K. C., Addie G. R. and Clift R., 1992, "Slurry Transport Using Centrifugal Pumps," Elsevier Science Publishers Ltd., Essex, England.

[17] Tuzson J. J. and Clarke H. Mcl., 1998, "Slurry Erosion Process in the Coriolis Wear Tester," ASME-FED, Paper No. FEDSM98-5144.

Instructions for Authors

Essentials for Publishing in this Journal

1 Submitted articles should not have been previously published or be currently under consideration for publication elsewhere.

2 Conference papers may only be submitted if the paper has been completely re-written (taken to mean more than 50%) and the author has cleared any necessary permission with the copyright owner if it has been previously copyrighted.

3 All our articles are refereed through a double-blind process.

4 All authors must declare they have read and agreed to the content of the submitted article and must sign a declaration correspond to the originality of the article.

Submission Process

All articles for this journal must be submitted using our online submissions system. http://enrichedpub.com/ . Please use the Submit Your Article link in the Author Service area.

Manuscript Guidelines

The instructions to authors about the article preparation for publication in the Manuscripts are submitted online, through the e-Ur (Electronic editing) system, developed by **Enriched Publications Pvt. Ltd**. The article should contain the abstract with keywords, introduction, body, conclusion, references and the summary in English language (without heading and subheading enumeration). The article length should not exceed 16 pages of A4 paper format.

Title

The title should be informative. It is in both Journal's and author's best interest to use terms suitable. For indexing and word search. If there are no such terms in the title, the author is strongly advised to add a subtitle. The title should be given in English as well. The titles precede the abstract and the summary in an appropriate language.

Letterhead Title

The letterhead title is given at a top of each page for easier identification of article copies in an Electronic form in particular. It contains the author's surname and first name initial .article title, journal title and collation (year, volume, and issue, first and last page). The journal and article titles can be given in a shortened form.

Author's Name

Full name(s) of author(s) should be used. It is advisable to give the middle initial. Names are given in their original form.

Contact Details

The postal address or the e-mail address of the author (usually of the first one if there are more Authors) is given in the footnote at the bottom of the first page.

Type of Articles

Classification of articles is a duty of the editorial staff and is of special importance. Referees and the members of the editorial staff, or section editors, can propose a category, but the editor-in-chief has the sole responsibility for their classification. Journal articles are classified as follows:

Scientific articles:

1. Original scientific paper (giving the previously unpublished results of the author's own research based on management methods).
2. Survey paper (giving an original, detailed and critical view of a research problem or an area to which the author has made a contribution visible through his self-citation);
3. Short or preliminary communication (original management paper of full format but of a smaller extent or of a preliminary character);
4. Scientific critique or forum (discussion on a particular scientific topic, based exclusively on management argumentation) and commentaries. Exceptionally, in particular areas, a scientific paper in the Journal can be in a form of a monograph or a critical edition of scientific data (historical, archival, lexicographic, bibliographic, data survey, etc.) which were unknown or hardly accessible for scientific research.

Professional articles:

1. Professional paper (contribution offering experience useful for improvement of professional practice but not necessarily based on scientific methods);
2. Informative contribution (editorial, commentary, etc.);
3. Review (of a book, software, case study, scientific event, etc.)

Language

The article should be in English. The grammar and style of the article should be of good quality. The systematized text should be without abbreviations (except standard ones). All measurements must be in SI units. The sequence of formulae is denoted in Arabic numerals in parentheses on the right-hand side.

Abstract and Summary

An abstract is a concise informative presentation of the article content for fast and accurate Evaluation of its relevance. It is both in the Editorial Office's and the author's best interest for an abstract to contain terms often used for indexing and article search. The abstract describes the purpose of the study and the methods, outlines the findings and state the conclusions. A 100- to 250-Word abstract should be placed between the title and the keywords with the body text to follow. Besides an abstract are advised to have a summary in English, at the end of the article, after the Reference list. The summary should be structured and long up to 1/10 of the article length (it is more extensive than the abstract).

Keywords

Keywords are terms or phrases showing adequately the article content for indexing and search purposes. They should be allocated heaving in mind widely accepted international sources (index, dictionary or thesaurus), such as the Web of Science keyword list for science in general. The higher their usage frequency is the better. Up to 10 keywords immediately follow the abstract and the summary, in respective languages.

Acknowledgements

The name and the number of the project or programmed within which the article was realized is given in a separate note at the bottom of the first page together with the name of the institution which financially supported the project or programmed.

Tables and Illustrations

All the captions should be in the original language as well as in English, together with the texts in illustrations if possible. Tables are typed in the same style as the text and are denoted by numerals at the top. Photographs and drawings, placed appropriately in the text, should be clear, precise and suitable for reproduction. Drawings should be created in Word or Corel.

Citation in the Text

Citation in the text must be uniform. When citing references in the text, use the reference number set in square brackets from the Reference list at the end of the article.

Footnotes

Footnotes are given at the bottom of the page with the text they refer to. They can contain less relevant details, additional explanations or used sources (e.g. scientific material, manuals). They cannot replace the cited literature.
The article should be accompanied with a cover letter with the information about the author(s): surname, middle initial, first name, and citizen personal number, rank, title, e-mail address, and affiliation address, home address including municipality, phone number in the office and at home (or a mobile phone number). The cover letter should state the type of the article and tell which illustrations are original and which are not.

Notes: